Synchrotron radiation-based X-ray techniques & cultural heritage objects: an integrated multi-material, multi-technique and multi-scale approach to study their composition and evolution

Letizia Monico

CNR-Institute of Chemical Sciences and Technologies "Giulio Natta" (SCITEC) (Perugia, Italy)

letizia.monico@cnr.it

CHANGES
CULTURAL HERITAGE ACTIVE INNOVATION FOR NEX-GEN SUSTAINABLE SOCIETY
EXTENDED PARTNERSHIP
Finanziato dall'Unione europea NextGenerationEU
Ministero dell'Università e della Ricerca
Italiadomani

SR-based X-ray methods for cultural heritage objects*

➢ **Cultural heritage objects**: heterogeneous and composite systems, in the most of cases composed of multiple layers, whose thickness can achieve values of a few micrometers.

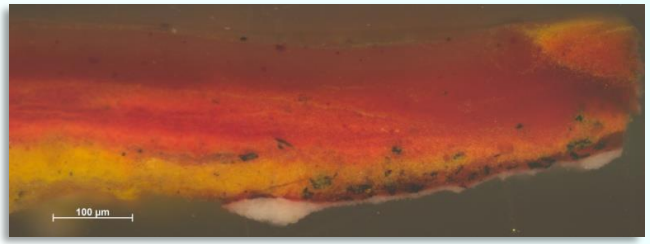

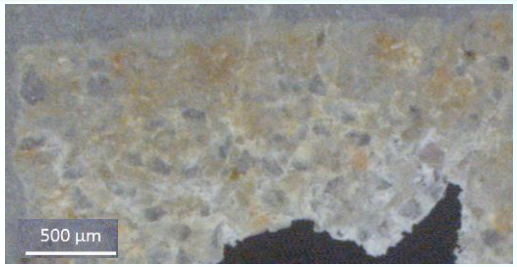

Subject to chemical transformations, often involving changes of the oxidation state of elements and formation of polymorphs.

➢ **SR-based X-ray methods (imaging/mapping and single-point analysis mode):** possibility of obtaining information about the chemical nature and distribution of different phases down to the sub-micrometer scale length.

a) **micro-X-ray fluorescence (µ-XRF)** for elemental microanalysis down to the sub-ppm level.

b) **micro-X-ray absorption spectroscopy (µ-XAS)** for probing the local chemical environment (oxidation state, coordination numbers, site symmetry and distortion, bond distances) of selected elements; it can be equally applied on amorphous or crystalline materials.

c) **micro-X-ray diffraction (µ-XRD)** for obtaining long range order information about the presence and nature of crystalline phases.

* M. Cotte *et al., Accounts of chemical research* 43 (2010) 705-714; L. Bertrand *et al., Appl. Phys. A* 106 (2012) 377–396; K. Janssens *et al., Annu. Rev. Anal. Chem.* 6 (2013) 399–425; K. Janssens *et al., Top. Curr. Chem.* 374(6) (2016), doi:10.1007/s41061-016-0079-2; M. Cotte *et al., JAAS* 32 (2017) 477–493; V. Gonzalez *et al., Chem. Eur. J.* 26 (2020) 1703 –1719; S. Quartieri, Synchrotron Radiation in Art, Archaelogy and Cultural Heritage. In *Synchrotron Radiation - Basics, Methods and Applications* (S. Mobilio, F. Boscehrini, C. Meneghini Eds.), Springer (2015), pp. 677-695.

Why SR for X-ray diffraction and spectroscopy?

- ***high X-ray flux.*** Fundamental requirement to obtain high signal-to-noise data in a reasonable time frame; parameter particularly critical if the element of interest is at low concentration in a sample. Synchrotron sources provide X-rays of five or more orders of magnitude greater flux than conventional laboratory X-ray sources.

- ***Broad spectral range at uniformly high flux.*** A typical XAS/XRF spectrum covers about 1000 eV. Tunable monochromators with appropriate d-spacings can be used to scan through a broad range of energy; thus, it is possible select the most appropriate energy range for an experiment.

- ***High stability in flux, energy and beam position.***

XANES/XRF/XRD experiments

Single point XAS analysis (XRF and TEY mode)

samples have to be allocated on a conductive material (e.g. carbon tape)

A) multiple energies elemental mapping: 2D µ-XRF

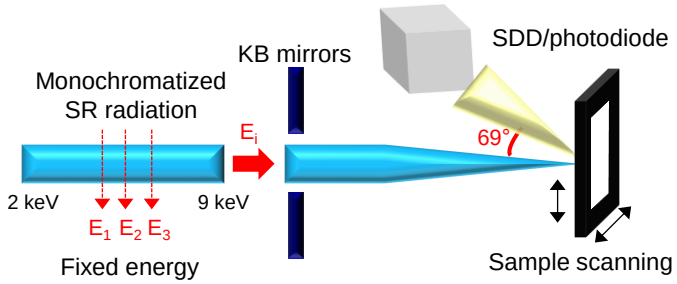

C) Chemical mapping: 2D µ-XANES (XRF mode)

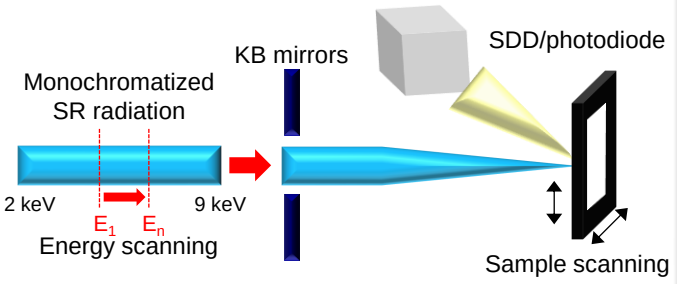

B) Single point µ-XANES analysis (XRF mode)

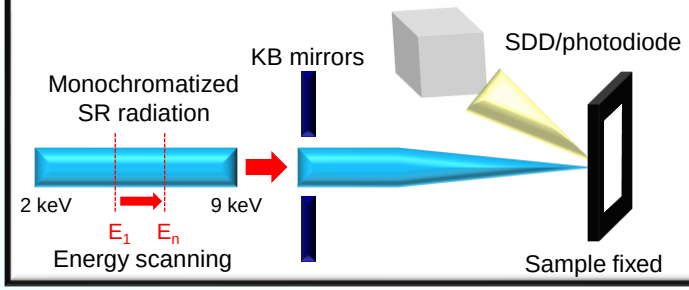

D) Chemical imaging: full-field (FF) XANES (transmission mode)

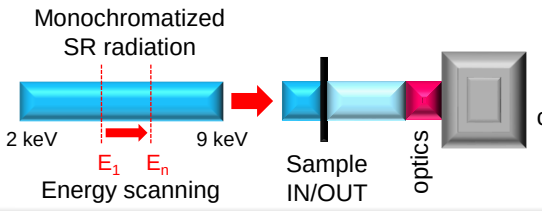

samples have to be analyzed as thin sections

2D µ-XRF/µ-XANES

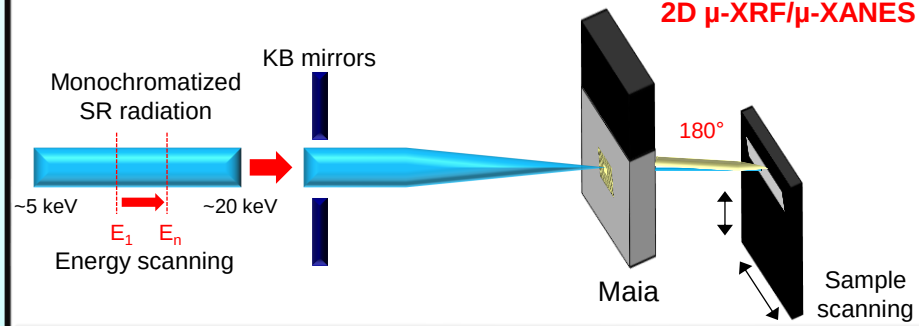

2D µ-XRD (transmission mode)

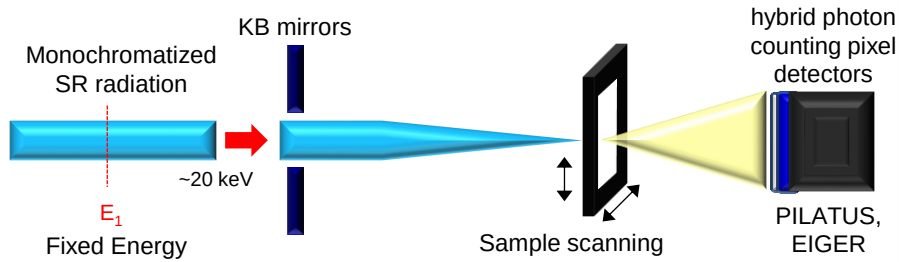

XANES/XRF mapping/imaging experiments

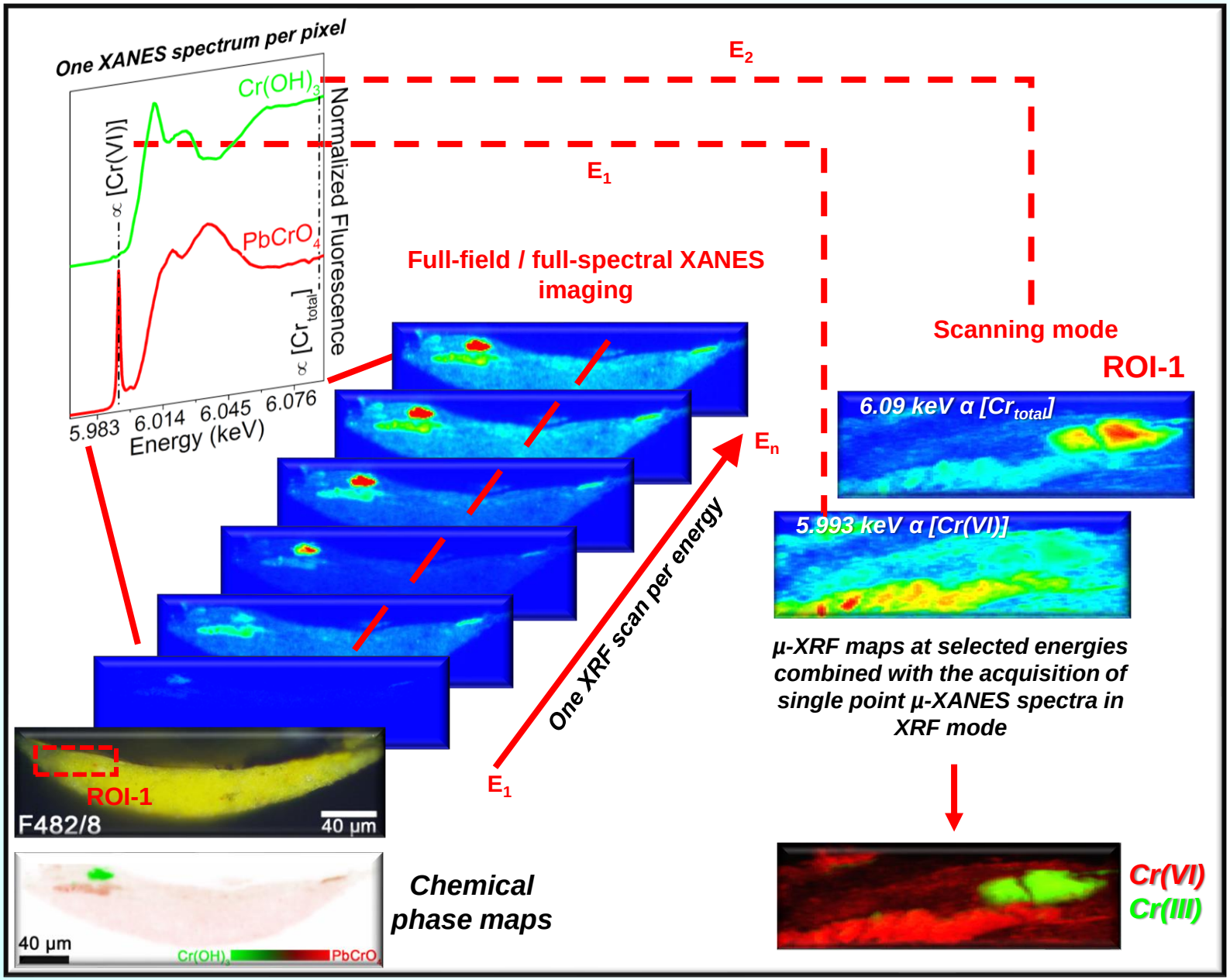

SR for Cultural heritage materials: further readings

Handbook of Cultural Heritage Analysis pp 45–67 | Cite as

Home > Handbook of Cultural Heritage Analysis > Reference work entry

X-Ray Absorption Spectroscopy (XAS) Applied to Cultural Heritage

Francesco D'Acapito

In: D'Amico, S., Venuti, V. (eds) Handbook of Cultural Heritage Analysis. Springer, Cham. https://doi.org/10.1007/978-3-030-60016-7_4

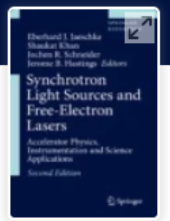

Synchrotron Light Sources and Free-Electron Lasers pp 2457–2483 | Cite as

Home > Synchrotron Light Sources and Free-Electron Lasers > Reference work entry

Using Synchrotron Radiation for Characterization of Cultural Heritage Materials

Koen Janssens & Marine Cotte

In: Jaeschke, E., Khan, S., Schneider, J., Hastings, J. (eds) Synchrotron Light Sources and Free-Electron Lasers. Springer, Cham. https://doi.org/10.1007/978-3-030-23201-6_78

Historical glasses

JPhys Photonics

PAPER • OPEN ACCESS

Unravelling the role of iron and manganese oxides in colouring Late Antique glass by micro-XANES and micro-XRF spectroscopies

To cite this article: Francesca Gherardi *et al* 2024 *J. Phys. Photonics* **6** 025001

JAAS

PAPER

View Article Online
View Journal | View Issue

CrossMark click for updates

Cite this: *J. Anal. At. Spectrom.*, 2015, 30, 642

Micro-XANES study on Mn browning: use of quantitative valence state maps

Gert Nuyts,*[a] Simone Cagno,[ab] Simone Bugani[c] and Koen Janssens[a]

Manufacturing process of Atlantic tradition glass*

experimental natron-type glass

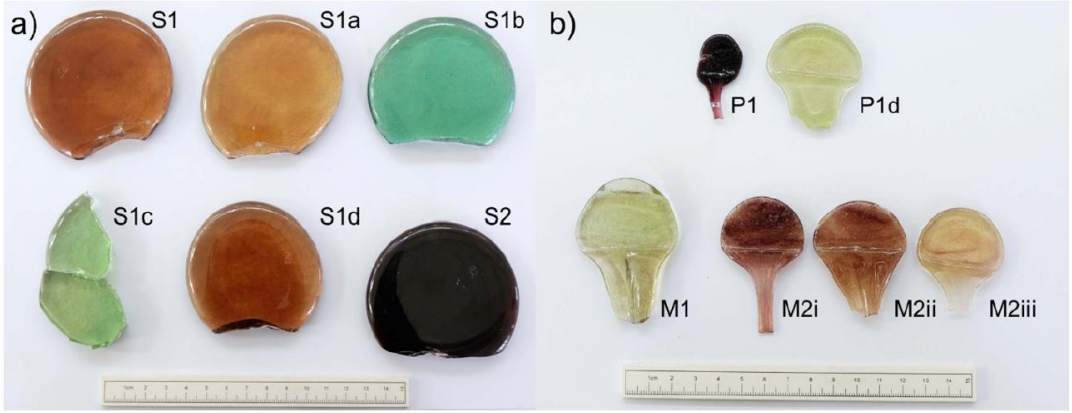

- The combined presence of **iron (Fe) and manganese (Mn)** produces glasses with a **wide range of colours (from green to amber to purple).**
- The colour depends on the relative amounts of Mn and Fe in different oxidation states

$$Fe(II)_{yellowish} + Mn(III)_{purplish} \rightleftharpoons Fe(III)_{bluish} + Mn(II)_{yellowish}$$

- Study of **lab-prepared/experimental natron-type glass** and **archaeological glass** from Tintagel and Whithorn (UK) (5th–7th century) by **Fe and Mn K-edge XANES/XRF spectroscopy** combined with UV-Visible spectroscopy and PCA to evaluate: *(1) the influence of different glass production parameters; (2) the variation of Fe and Mn oxidation states; (3) the optical character.*

Archaeological glass (Tintagel/Whithorn, 5th–7th century)

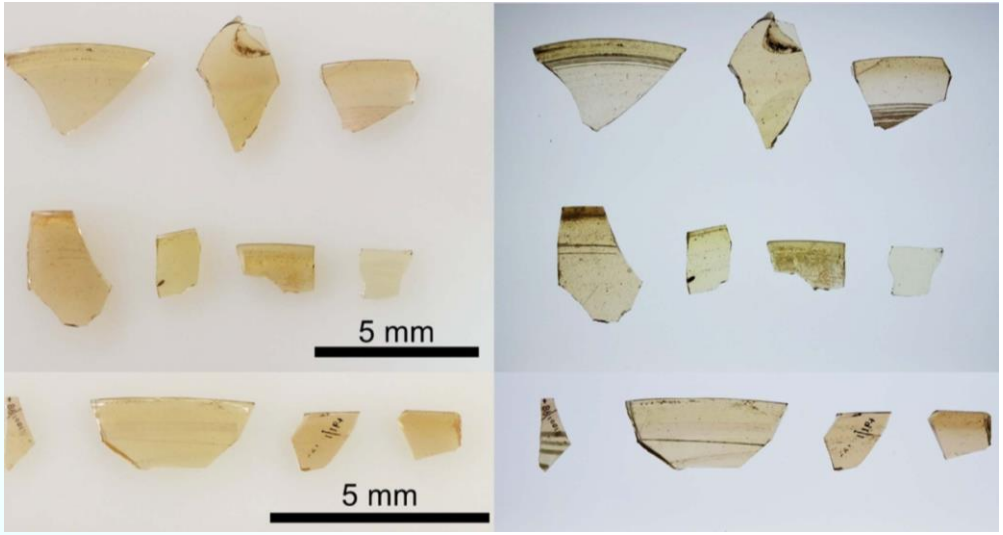

reflected light ***transmitted light***

*F. Gheradi *et al., J. Phys. Photonics* 6 (2024) 025001, https://doi.org/10.1088/2515-7647/ad2259

Manufacturing process of Atlantic tradition glass*

Fe K-edge XANES

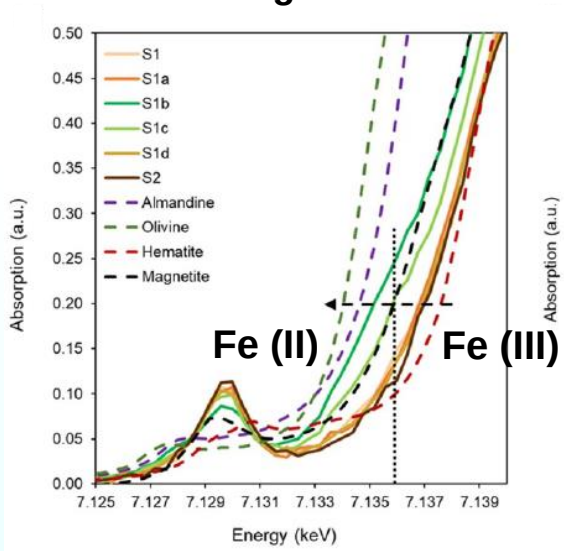

Mn K-edge XANES

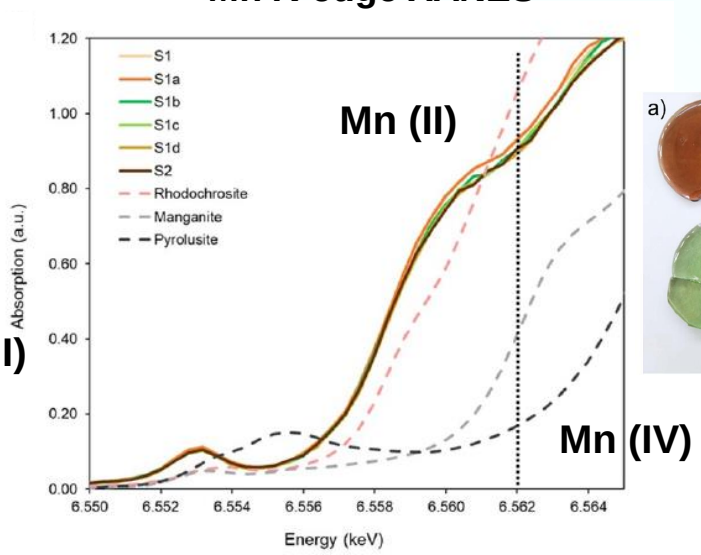

experimental natron-type glass

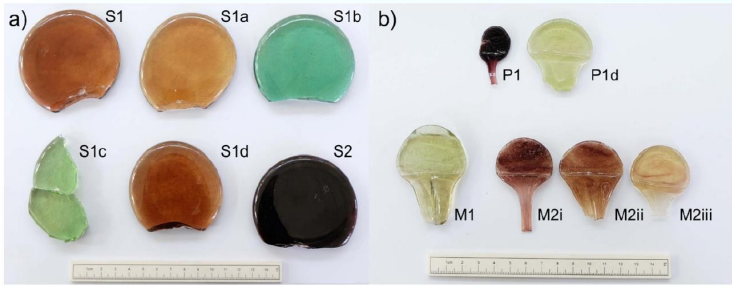

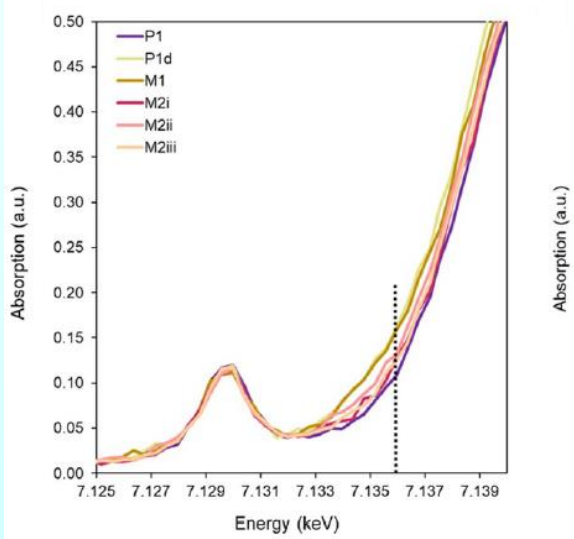

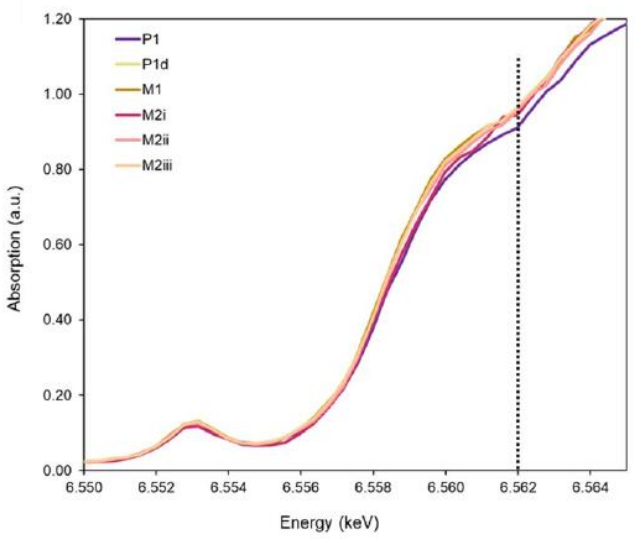

- ***Brown, amber, purple-coloured glasses:*** lowest content of yellowish Mn(II) and Fe(II) species;
- ***Purple coloured-glasses:*** increasing amount or Mn(III) species:
- ***Green-coloured glasses:*** increasing contribution of Fe(II) species

ESRF

ID21 beamline

*F. Gheradi *et al., J. Phys. Photonics* 6 (2024) 025001, https://doi.org/10.1088/2515-7647/ad2259

Manufacturing process of Atlantic tradition glass*

Fe K-edge XANES

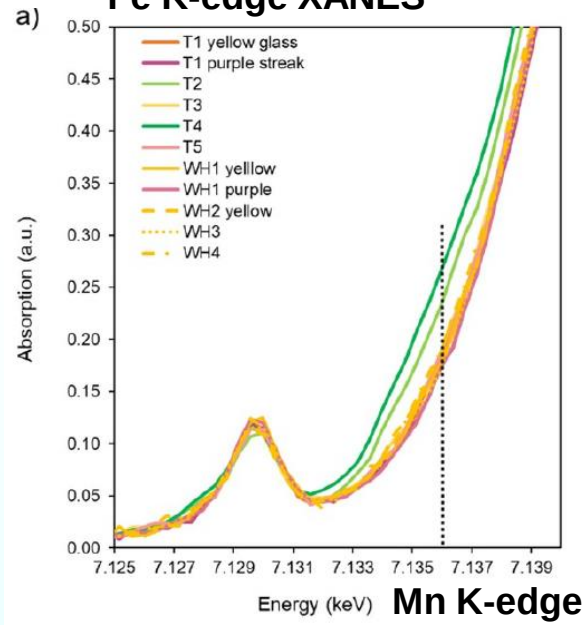

Archaeological glass (Tintagel/Whithorn, 5th–7th century)

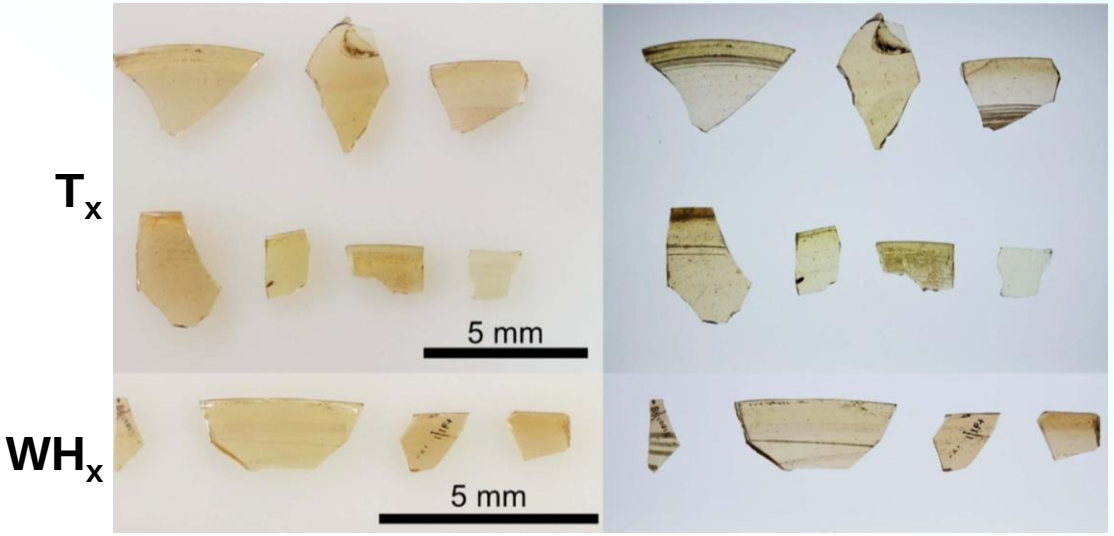

Mn K-edge XANES

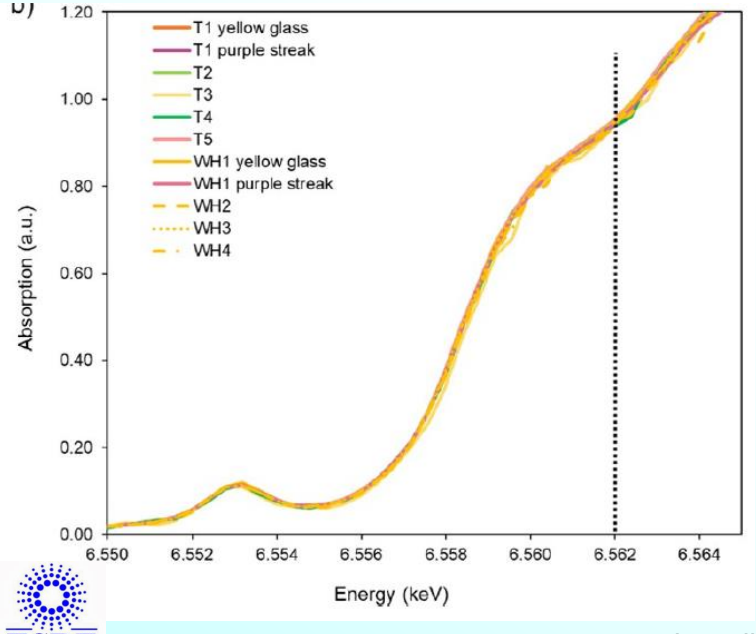

- The Atlantic West glass was probably made by remelting green glass [green being richer in Fe(II) than yellow glass] with some purple fragments [richer in Mn(III)].
- This would explain the remnants of purple streaks in some of the amber archaeological glass, which remain due to incomplete mixing of the melt.

*F. Gheradi *et al., J. Phys. Photonics* 6 (2024) 025001, https://doi.org/10.1088/2515-7647/ad2259

Glass corrosion: Mn K-edge μ-XANES/μ-XRF

- **Medieval glass**, can undergo **corrosion** due to the formation of **dark-coloured manganese-rich inclusions** that reduce the transparency of the glass.

- the presence of water and oxygen, **Mn(II) and/or Mn (III)** ions can be **oxidised** to higher oxidation states giving rise to, for example, insoluble **Mn(IV) compounds** (e.g., MnO_2) that can precipitate, a process favoured in alkaline conditions.

- Two different **restoration strategies** to improve the transparency: *(i) reduction of highly oxidised black/brown compounds using mildly reducing solutions; (ii) extraction of manganese from the inclusions by the application of chelating agents.*

- **Mn K-edge XANES/XRF mapping** to evaluate the effect of reducing treatments on historical glass, dated to the 14th century and originating from Sidney Sussex College (Cambridge, UK), suffering from manganese browning.

JAAS

PAPER

View Article Online
View Journal | View Issue

CrossMark click for updates

Cite this: *J. Anal. At. Spectrom.*, 2015, 30, 642

Micro-XANES study on Mn browning: use of quantitative valence state maps

Gert Nuyts,*[a] Simone Cagno,[ab] Simone Bugani[c] and Koen Janssens[a]

Glass corrosion: Mn K-edge XANES spectroscopy*

ESRF

ID21 beamline

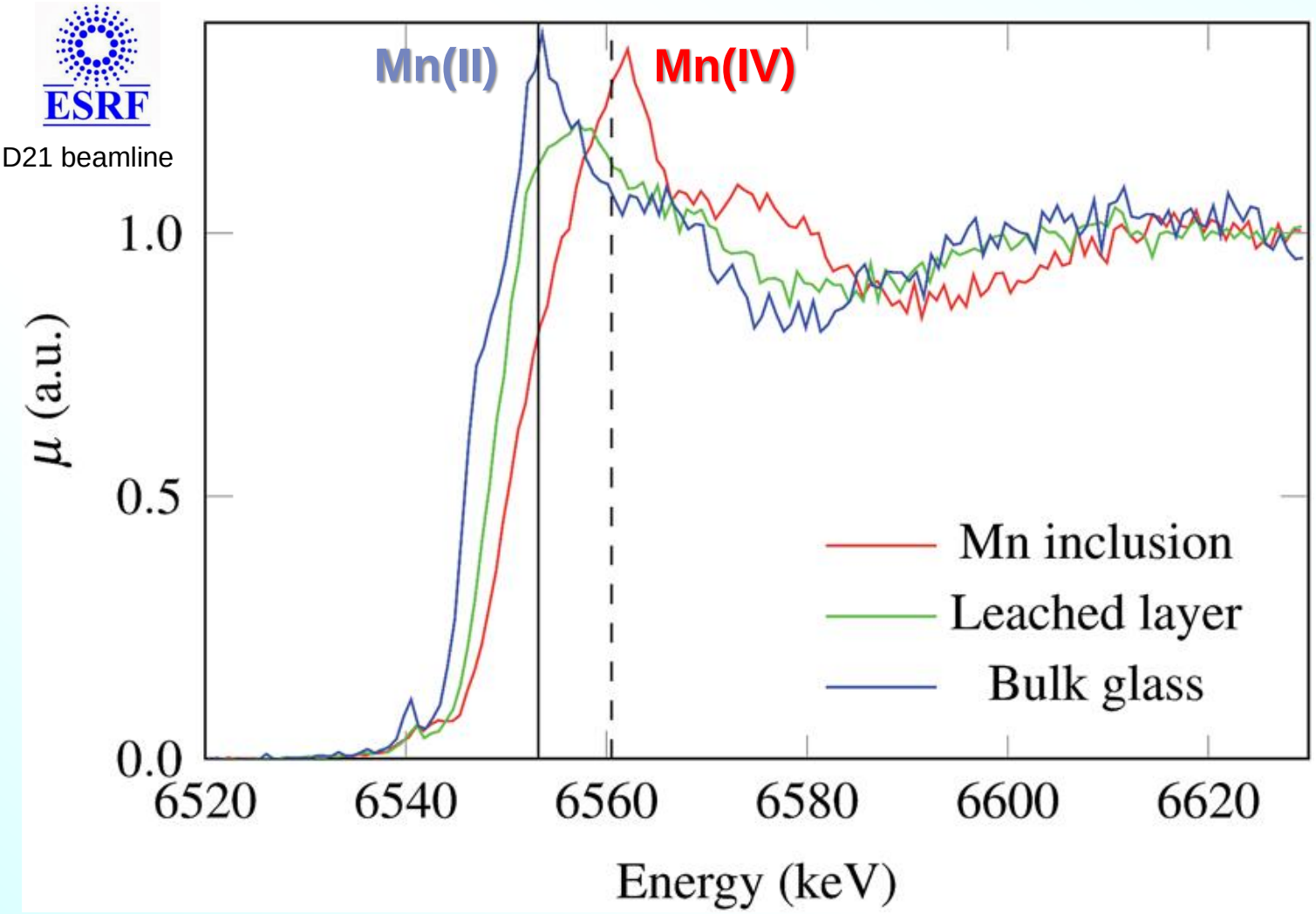

μ-XRF maps at selected energies for visualizing different oxidation states of manganese

*G. Nuyts *et al.*, JAAS 30 (2015), 642–650.

Glass corrosion: Mn oxidation state mapping*

ESRF
ID21 beamline

5% w/w hydroxylamine hydrochloride solution for 30 min

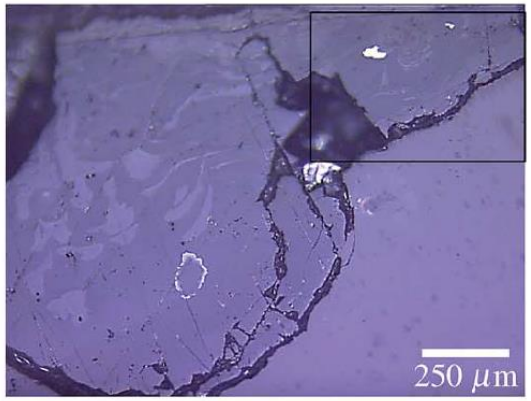

untreated

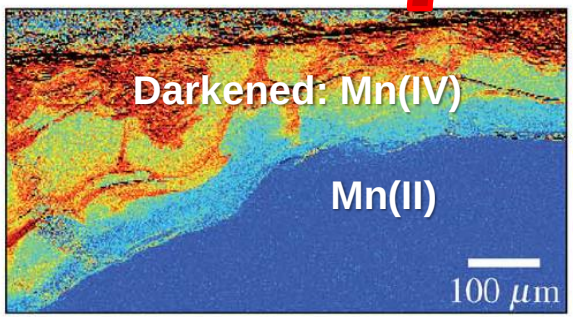

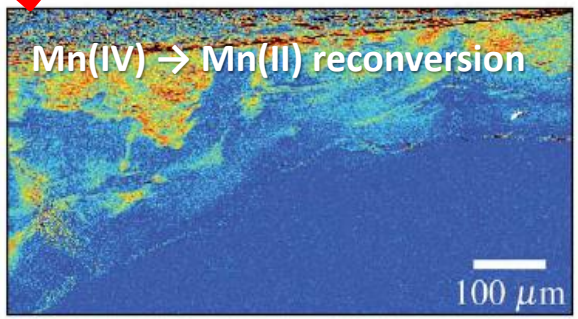

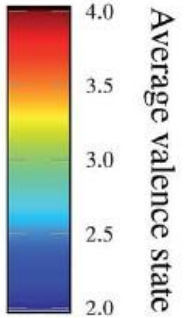

untreated

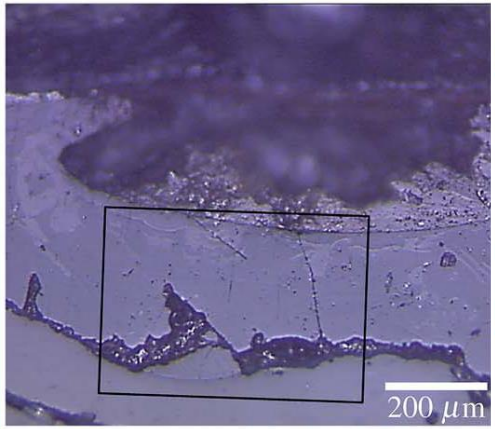

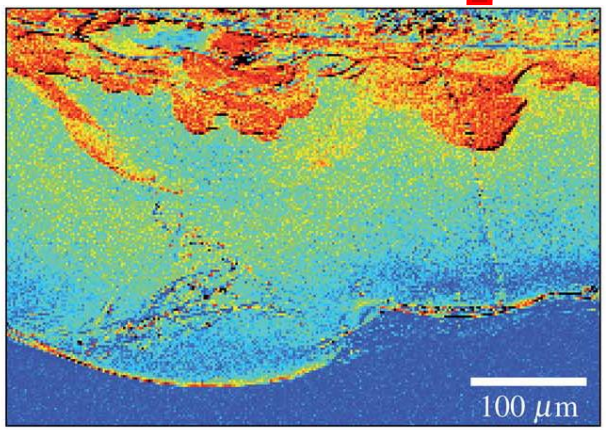

5% w/w citric acid for 30 min.

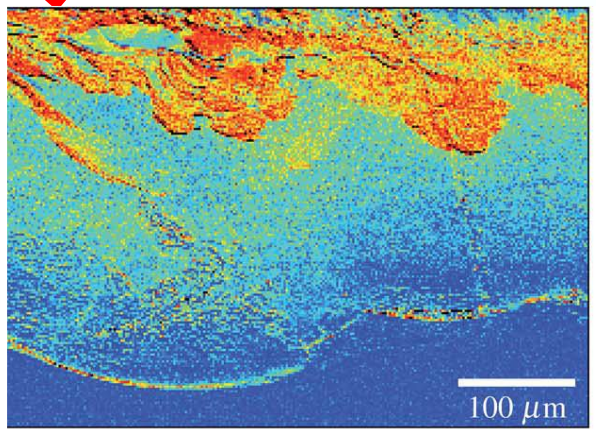

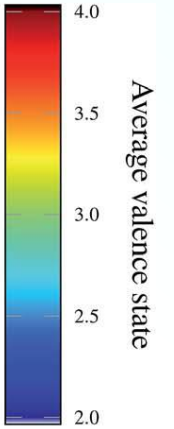

➢**The hydroxylamine treatment** proved to be the **most effective in reducing the highly oxidised Mn compounds** in the inclusions, a change that could be observed visually and was supported by Mn oxitation state mapping.

➢ **Preliminary radiation damage tests:** aimed at minimizing the photo-reduction of Mn(IV) to Mn(II) induced by the exposure to the X-ray beam.

*Figures re-adapted from G. Nuyts *et al.*, JAAS 30 (2015), 642–650.

Manufacturing process of Roman ceramics*

- **Black/red colour:** the **glossy black** contains significant amounts of **Fe(II),** while the **red ochre ground** is composed almost entirely of **Fe(III);**
- Produced from clays with very similar bulk chemistry but by manipulation of Fe oxidation state and mineralogy through skilled control of nanoscale porosity, kiln temperatures and oxidative environment.

- Study of **two fragments of roman ceramics**, from two different locations and times:

(i) B type Campanian ceramic: it has a high black gloss coating with a red non-vitrified body (found during the excavations of the old city of Narbonne and dated to the 1st century BCE).

(ii) Pre-sigillata fragment (La Graufesenque workshop; Millau, France - Augustan period): its paste is non-vitrified and has a red/brown colour while its slip is black. The slip is vitrified but not as brilliant as that of the Campanian ceramic.

- Phase studies by **full-filed XANES imaging at Fe K-edge**

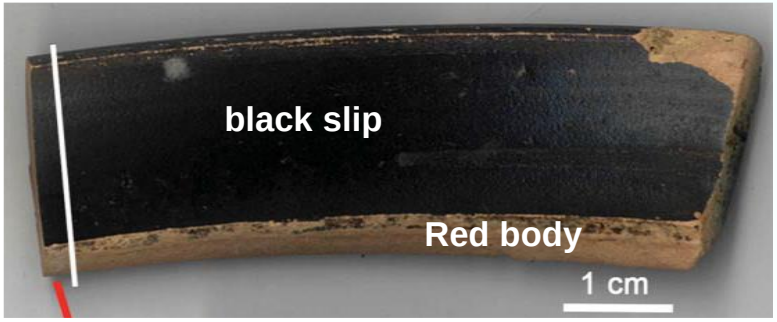

JAAS

RSC Publishing

PAPER

View Article Online
View Journal | View Issue

Cite this: *J. Anal. At. Spectrom.*, 2013, **28**, 1870

Full-field XANES analysis of Roman ceramics to estimate firing conditions—A novel probe to study hierarchical heterogeneous materials

Florian Meirer,[a] Yijin Liu,[b] Emeline Pouyet,[c] Barbara Fayard,[c] Marine Cotte,[c] Corinne Sanchez,[d] Joy C. Andrews,[b] Apurva Mehta[b] and Philippe Sciau*[e]

Manufacturing process of Roman ceramics*: Full field-XANES imaging at Fe K-edge

ESRF ID21 beamline

SLAC NATIONAL ACCELERATOR LABORATORY SSRL BL 6-2c

Pre-sigillata

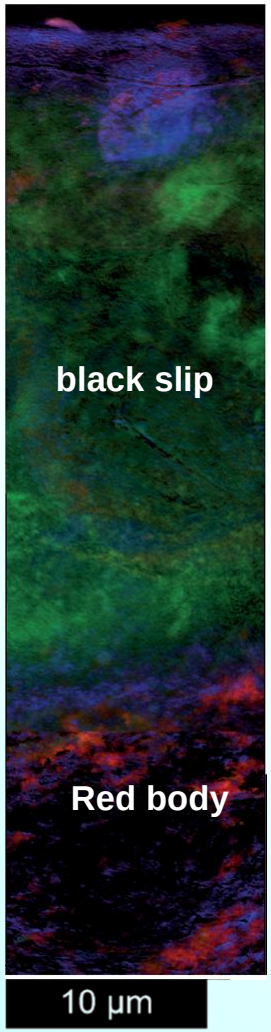

B type Campanian

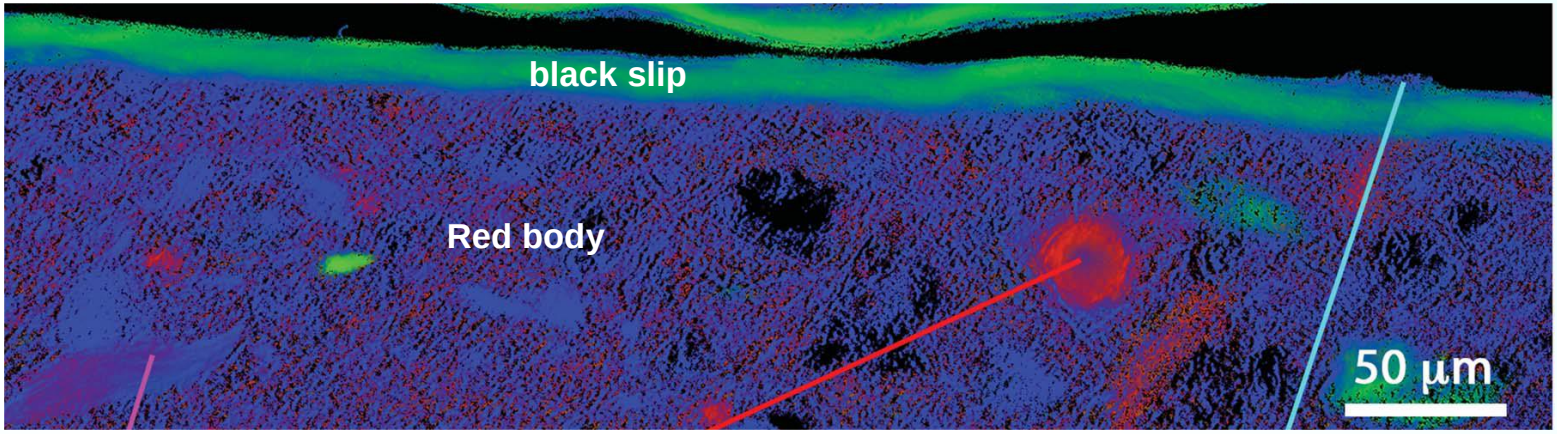

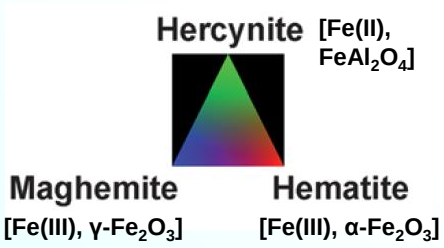

- Three mineral phases of Fe: hercynite [black, Fe(II)], hematite and maghemite [both red, Fe(III)]
- Very thin thicker and more uniform layer on the Pre-sigillata slip. Two possible explanations: (i) the surface layer was polished away after firing; (ii) the surface of the slip was protected from oxygen during reoxidation and the vessel oxidized from the inside out.
- Pre-sigillata appears to be mostly hematite while that of the Campanian is mostly maghemite with a few large islands of hematite;

The final re-oxidation step of the three stage firing protocol (oxidative→reductive→oxidative) for the Campanian ceramic was performed under either lower oxygen fugacity or at significantly lower temperature and/or shorter duration than the Pre-sigillata ceramic.

* F. Merier *et al.*, J. Anal. At. Spectrom. 28 (2013), 1870–1883.

Stone materials – consolidation treatments

Contents lists available at ScienceDirect

Materials Characterization

journal homepage: www.elsevier.com/locate/matchar

Materials Characterization 156 (2019) 109853

Inspecting adhesion and cohesion of protectives and consolidants in sandstones of architectural heritage by X-ray microscopy methods

Simona Raneri[a,*], Alessandra Giannoncelli[b], Elisabeth Mascha[c], Lucia Toniolo[d], Marco Roveri[d], Andrea Lazzeri[e,f], Maria Beatrice Coltelli[e,f], Luca Panariello[e,f], Marco Lezzerini[a], Johannes Weber[c]

Analytical Methods

ROYAL SOCIETY OF CHEMISTRY

PAPER

View Article Online
View Journal | View Issue

Check for updates

Cite this: *Anal. Methods*, 2020, **12**, 1587

Synchrotron radiation μ X-ray diffraction in transmission geometry for investigating the penetration depth of conservation treatments on cultural heritage stone materials

Elena Possenti, *[a] Claudia Conti, [a] G. Diego Gatta, [b] Marco Merlini, [b] Marco Realini [a] and Chiara Colombo [a]

OPEN

SCIENTIFIC REPORTS

nature research

(2020) 10:14337

Synchrotron radiation Ca K-edge 2D-XANES spectroscopy for studying the stratigraphic distribution of calcium-based consolidants applied in limestones

Letizia Monico[1,2✉], Laura Cartechini[1✉], Francesca Rosi[1], Wout De Nolf[3], Marine Cotte[3,4], Riccardo Vivani[5], Celeste Maurich[1] & Costanza Miliani[6]

*Ca speciation investigations for probing the carbonatation process of Ca-based consolidants into limestones**

CONTEXT

- Application of consolidants: common practice for the preservation of limestones used in archaeological/historical monuments against outdoor weathering.
- Recently, inorganic treatments involving the in situ formation of $CaCO_3$ have been proposed, being more suitable due to their higher compatibility and stability with respect to synthetic polymers.

RESEARCH PROBLEM

- Main issue of Ca-based consolidants: formation of different $CaCO_3$ phases: **amorphous $CaCO_3$ (ACC)** deposits and crystalline systems composed of either **vaterite, or calcite, or their mixtures**.
- The formation of different phases of $CaCO_3$ is relevant because it may have implications on the long-term performance of a consolidation treatment.

MATERIALS and TREATMENTS

- Substrate: high porosity limestone (Lecce stone, with porosity of ~37%).
- Treated stones cured with calcium acetoacetate (CaAcAc) under different RH% conditions (50, 80 and 95%) and at 40°C.
- Analysis performed on “thin” cross-sections of treated substrate fragments (sizes of *ca.* 2×6 mm^2) embedded into resin and polished down to a thickness of *ca.* 150 μm.

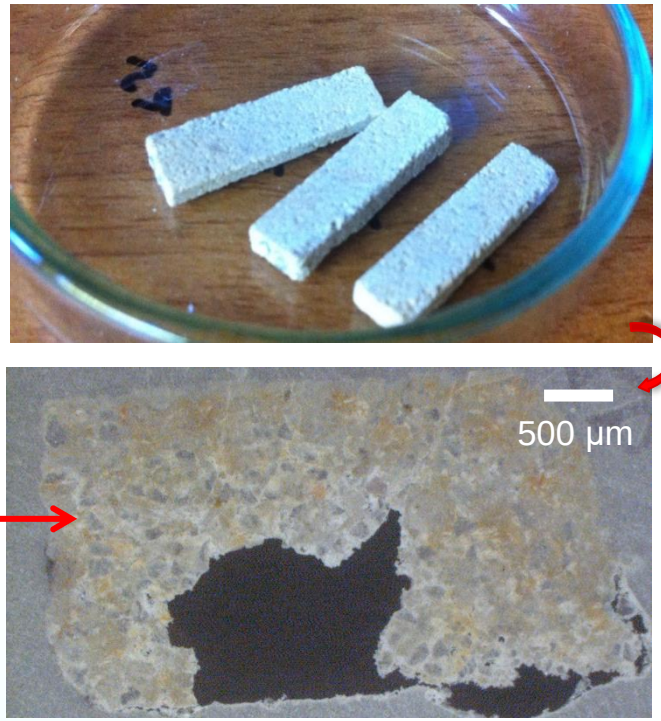

* L. Monico *et al., Scientific Reports* (2020) 10:14337, https://doi.org/10.1038/s41598-020-71105-8

Why XANES spectroscopy at Ca K-edge?

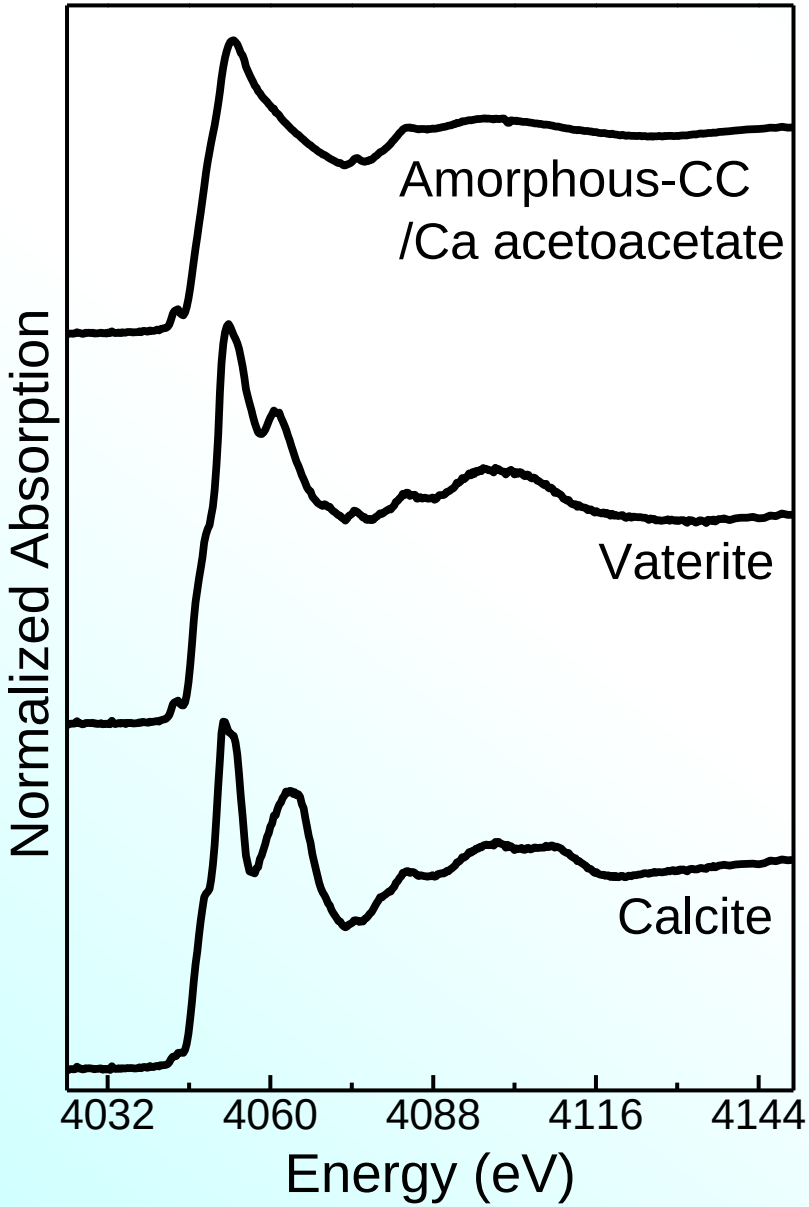

ESRF
ID21 beamline

High-specificity/sensitivity to distinguish 3 different forms of $CaCO_3$ (including the amorphous one)

Possibility to follow the kinetic of transformation and distribution of each phases within the limestone-substrate

* L. Monico *et al., Scientific Reports* (2020) 10:14337, https://doi.org/10.1038/s41598-020-71105-8

Ca K-edge FF-XANES imaging*

ESRF
ID21 beamline

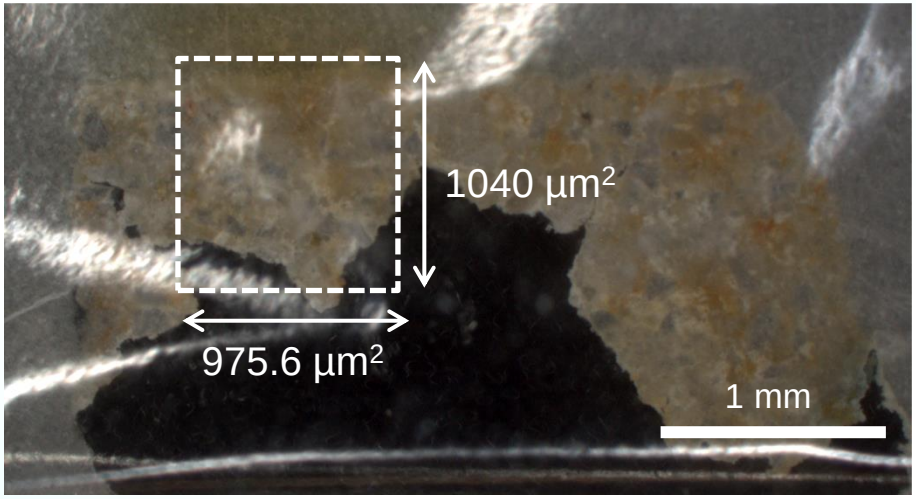

EXPERIMENTAL ISSUE:

Large (ca. 2×6 mm²) and heterogeneous samples.

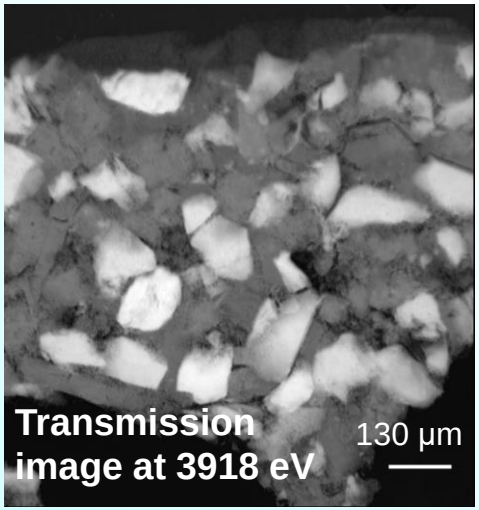

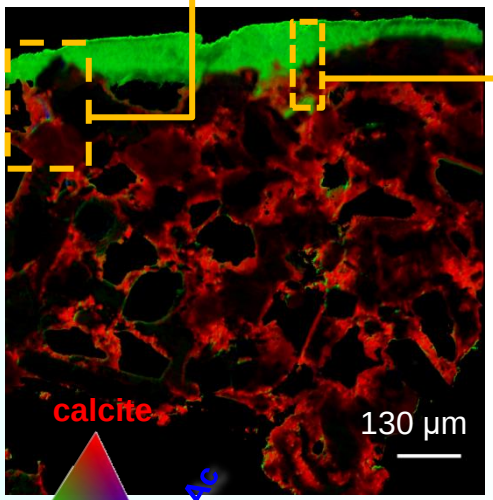

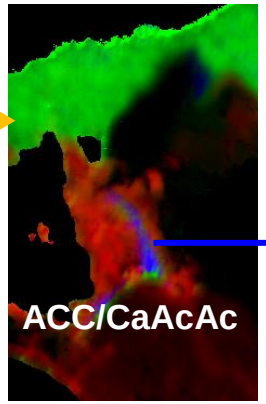

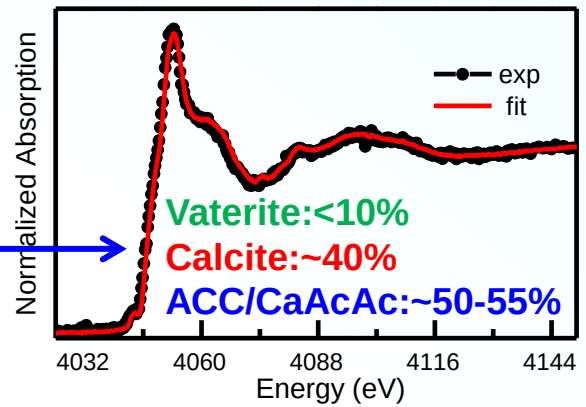

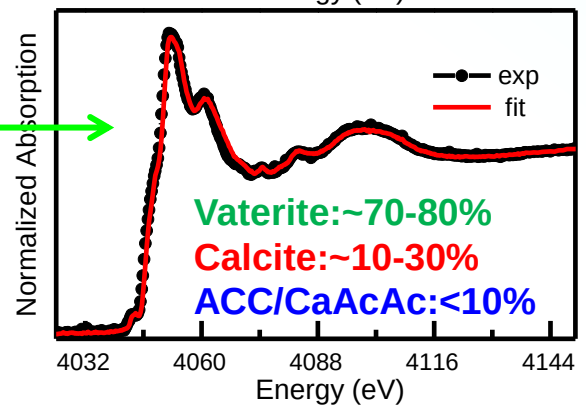

Step size (h×v): 0.65×0.65 µm²
Total acquisition time (549 energies): ~5 h:40 min
Time per energy: 37.8 s

* L. Monico *et al.*, *Scientific Reports* (2020) 10:14337, https://doi.org/10.1038/s41598-020-71105-8

Ca K-edge FF-XANES imaging/2D µ-XRD mapping*

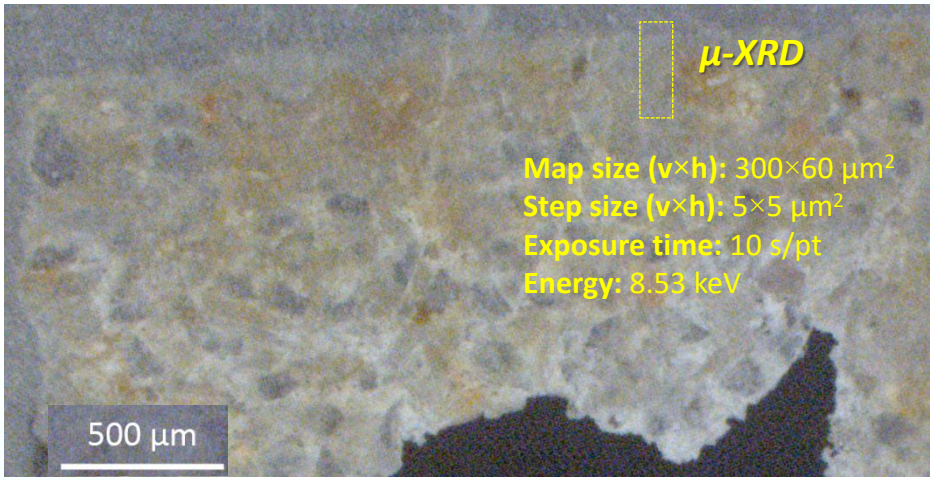

Ca K-edge FF-XANES imaging

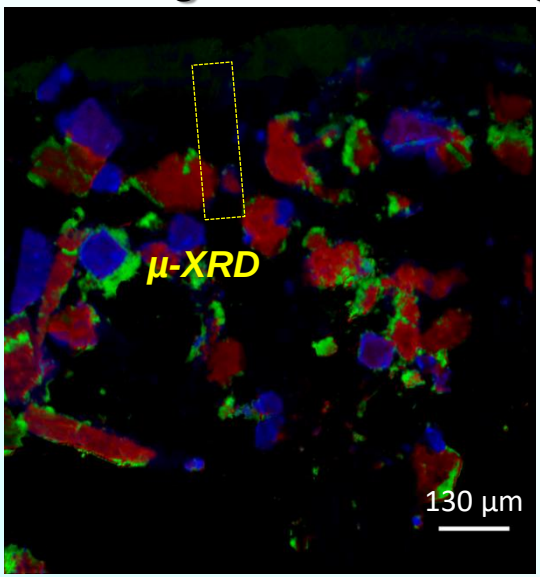

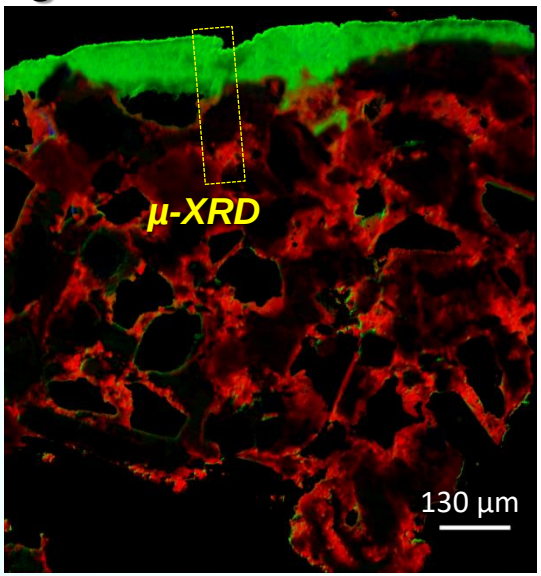

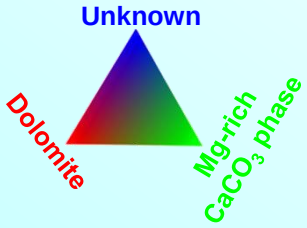

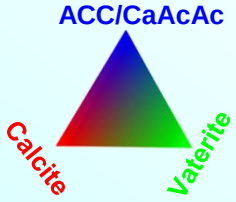

ESRF
ID21 beamline

2D µ-XRD mapping

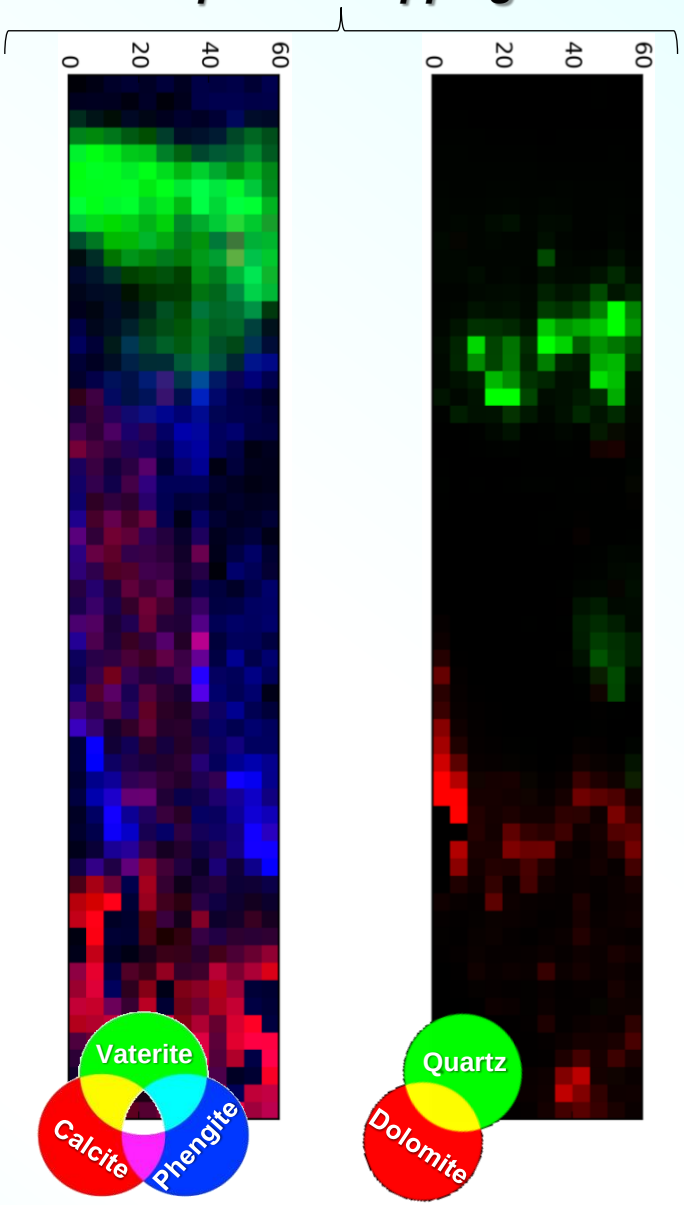

* L. Monico *et al.*, *Scientific Reports* (2020) 10:14337, https://doi.org/10.1038/s41598-020-71105-8

Lead calcium phosphate solid solutions: alteration compounds or original materials?

The presence of lead-calcium phosphates on artworks is not clear. It might be caused by:

- Intentional use as pigment or filler;
- A result of alteration processes of original materials.

Hydroxyapatite [$Ca_5(PO_4)_3OH$] can immobilize lead, thus producing a solid solution of $Pb_xCa_{(5-x)}(PO_4)_3OH$ where Pb(II) ions mostly occupy Ca(II) sites.

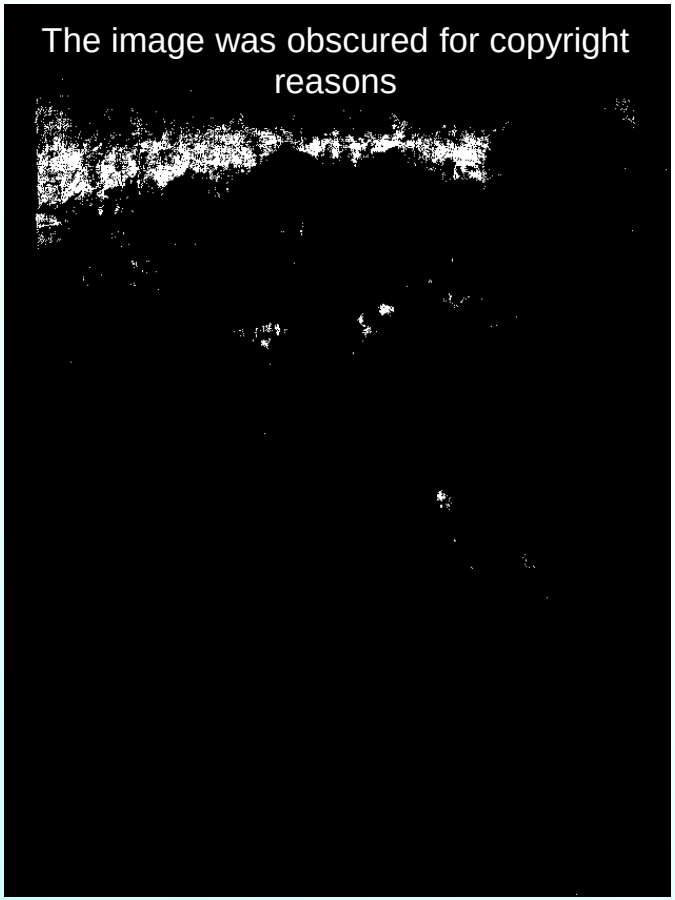

Pyromorphite $[Pb_5(PO_4)_3(OH)]$ and/or Phosphohedyphane $[(Pb,Ca)_5(PO_4)_3Cl]$?

Lead calcium phosphate solid solutions: synthesis and characterization

$$5M^{2+} + 3PO_4^{3-} + OH^- \Rightarrow Pb_xCa_{(5-x)}(PO_4)_3OH$$

M = Ca, Pb, (Ca+Pb)

X_{Pb}

Samples	Formula	Ca:Pb Ratio
HA	$Ca_5(PO_4)_3OH$	1 : 0
PbHA-10	$(Pb_{0.1}Ca_{0.9})_5(PO_4)_3OH$	0.9 : 0.1
PbHA-20	$(Pb_{0.2}Ca_{0.8})_5(PO_4)_3OH$	0.8 : 0.2
PbHA-40	$(Pb_{0.4}Ca_{0.6})_5(PO_4)_3OH$	0.4 : 0.6
PbHA-50	$(Pb_{0.5}Ca_{0.5})_5(PO_4)_3OH$	0.5 : 0.5
PbHA-70	$(Pb_{0.7}Ca_{0.3})_5(PO_4)_3OH$	0.3 : 0.7
PbHA-80	$(Pb_{0.8}Ca_{0.2})_5(PO_4)_3OH$	0.2 : 0.8
HPy	$Pb_5(PO_4)_3OH$	0 : 1

Analytical characterization of powders:

- Morphological, microstructural, and local atomic structure: SEM, XRD, XANES spectroscopy at Ca K- and P K-edges.
- further information on the molecular structure: FT-IR and Raman spectroscopies.

Applied Spectroscopy

Special Issue

Applied Spectroscopy
1–14
© The Author(s) 2024
Article reuse guidelines:
sagepub.com/journals-permissions
DOI: 10.1177/00037028241243375
journals.sagepub.com/home/asp
Sage

Non-Destructive and Non-Invasive Approaches for the Identification of Hydroxy Lead–Calcium Phosphate Solid Solutions ($(Pb_xCa_{1-x})_5(PO_4)_3OH$) in Cultural Heritage Materials

Claudio Costantino[1,2], Letizia Monico[1,2,3], Francesca Rosi[2], Riccardo Vivani[4], Aldo Romani[1,2], Luis Carlos Colocho Hurtarte[5,*], Eduardo Villalobos-Portillo[5,†], Christoph J. Sahle[5], Thomas Huthwelker[6], Catherine Dejoie[5], Manfred Burghammer[5], and Marine Cotte[5,7]

Lead calcium phosphate solid solutions: IR, Raman & XRD*

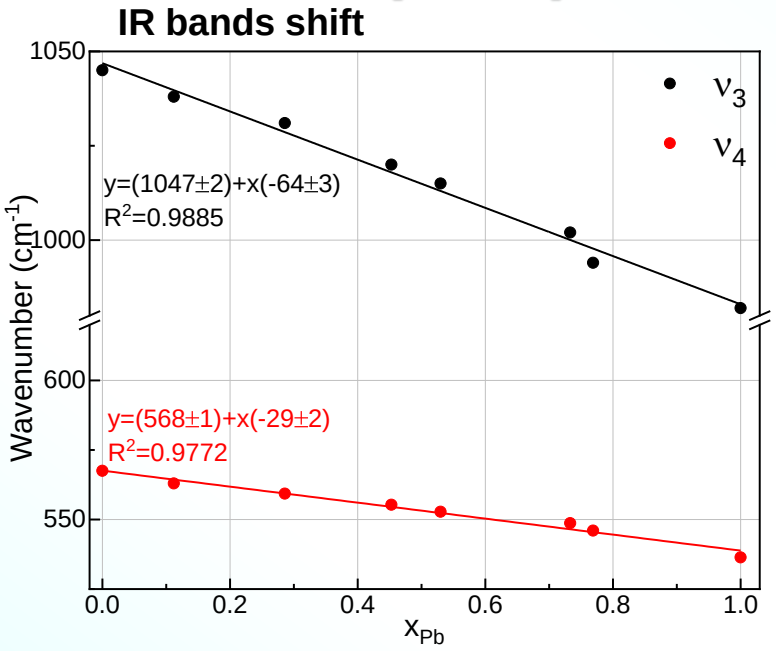

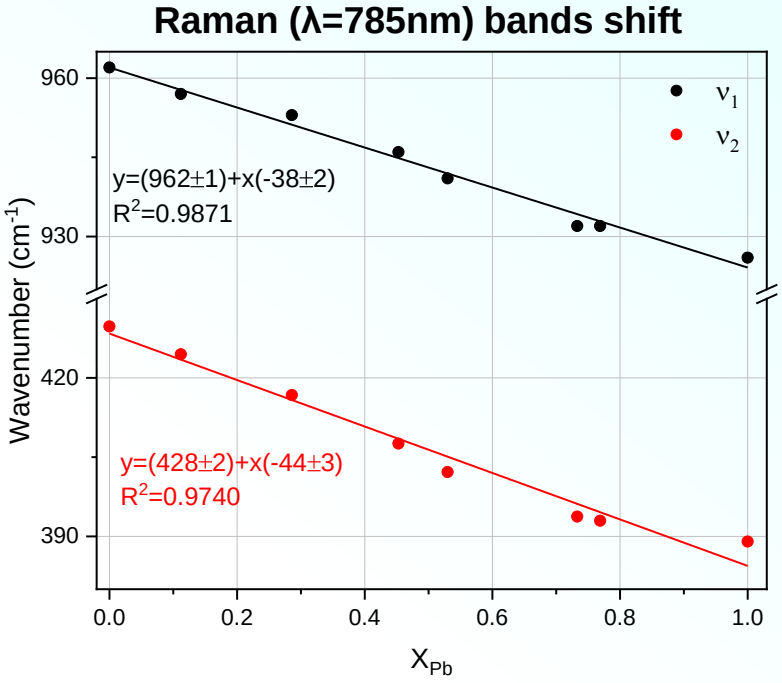

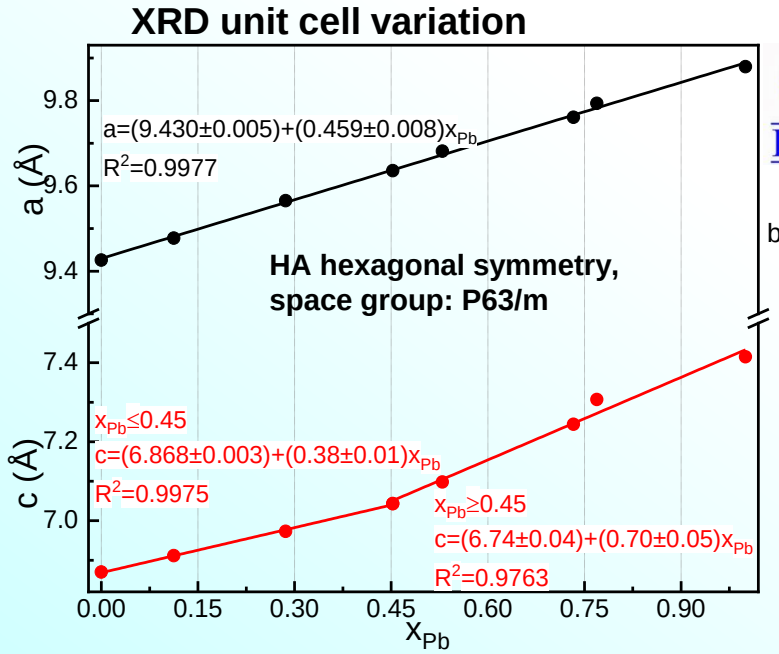

ESRF

ID22 beamline

- The substitution of lighter Ca^{2+} ions with heavier Pb^{2+} ions leads to the HA lattice expansion;
- This is the main responsible for the changes observed in the position, shape, width, and intensity of ν_3/ν_4 and ν_1/ν_2 FT-IR and Raman bands (stretching/bending of phosphate group)

* C. Costantino *et al.*, *Applied Spectroscopy* (2024), 00037028241243375

Lead calcium phosphate solid solutions: Ca K-/P K-edge XANES *

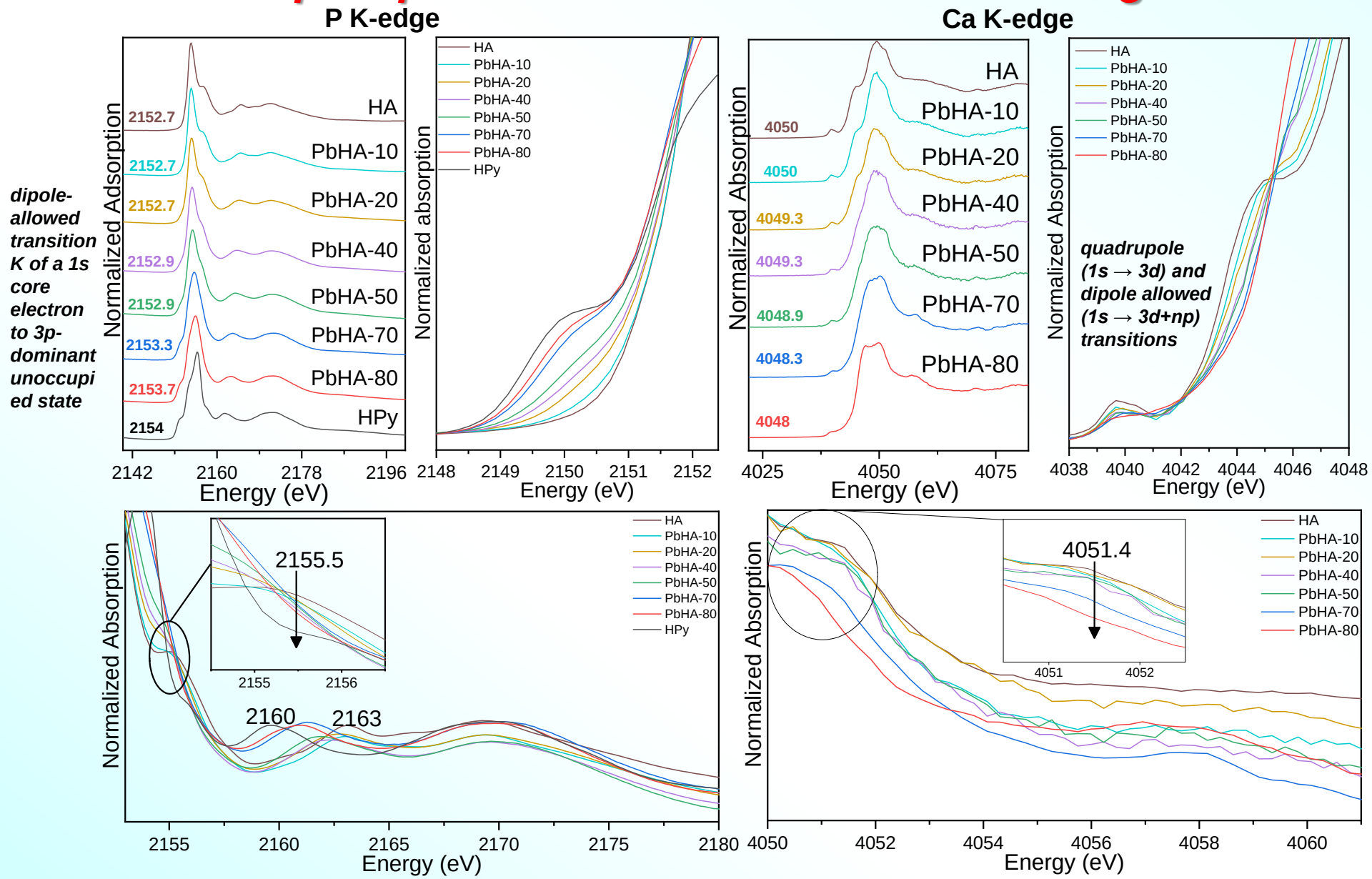

White line and band shape and energy position of pre-/post-edge signals of the P K-/Ca K-edge XANES spectra suitable as markers for the non-destructive discrimination of different PbHA-X compounds at the microscale.

* C. Costantino *et al., Applied Spectroscopy* (2024), 00037028241243375

Color changes in paintings: alteration of blue pigments

Fe K-and Co K-edges XAS analysis for the study of the fading of Prussian blue and discoloration of smalt

Fading of Prussian blue

➢ ***Prussian blue:*** discovered at the beginning of 18th century and of composition $MFe^{III}[Fe^{II}(CN)_6]\cdot xH_2O$ (with M= K^+, NH_4^+ or Na^+). The intense blue color arises from an intervalent electron transfer between the Fe(II) and Fe(III) oxidation states when light is absorbed at about 700 nm.

➢ Artificially aged model samples before and after light exposure have been investigated using a combination of Fe K-edge XAS analysis and iron-57 Mössbauer spectroscopy for the understanding of the alteration mechanism of this pigment.[(a)]

Artificially aged oil paint models

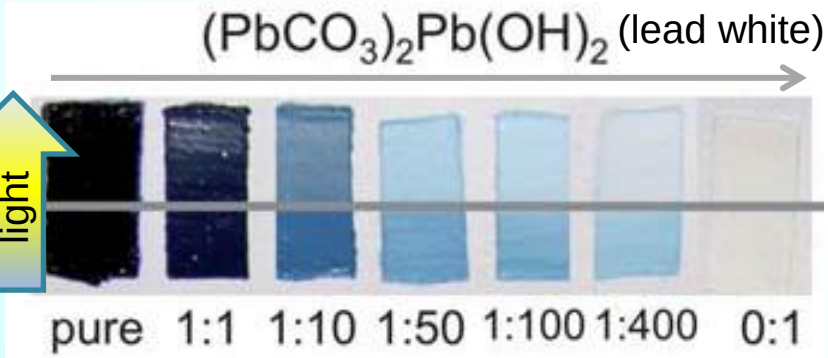

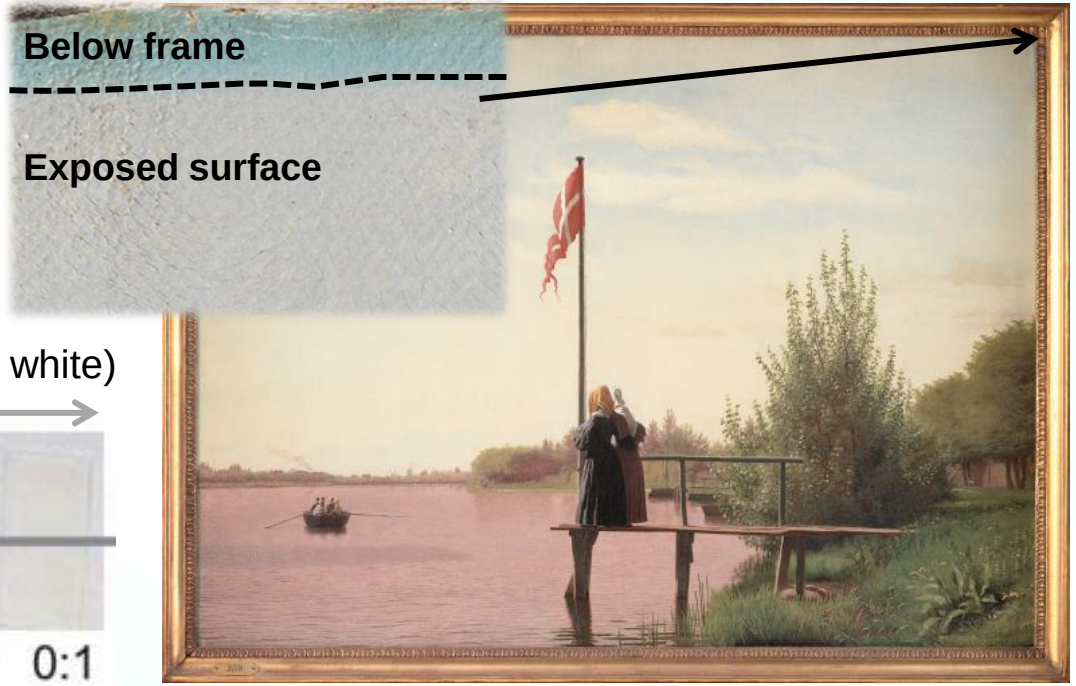

View of Lake Sortedam from Dosseringen Looking Towards the Suburb Nørrebro outside Copenhagen (1838, Christen Købke; Statens Museum for Kunst, Copenhagen, DK).[(b)]

[(a)] L. Samain et *al.,* J. Anal. At. Spectrom. 26 (2011) 930-941; L. Samain *et al.,* J. Anal. At. Spectrom. 28 (2013) 524–535. [(b)] A. Vila *et al.,* in: "Science and Art: The Painted Surface" (Eds: A. Sgamellotti, B. G. Brunetti, C. Miliani), The Royal Society of Chemistry, London, 2014, 354-372.

Fe K-edge XAS analysis*

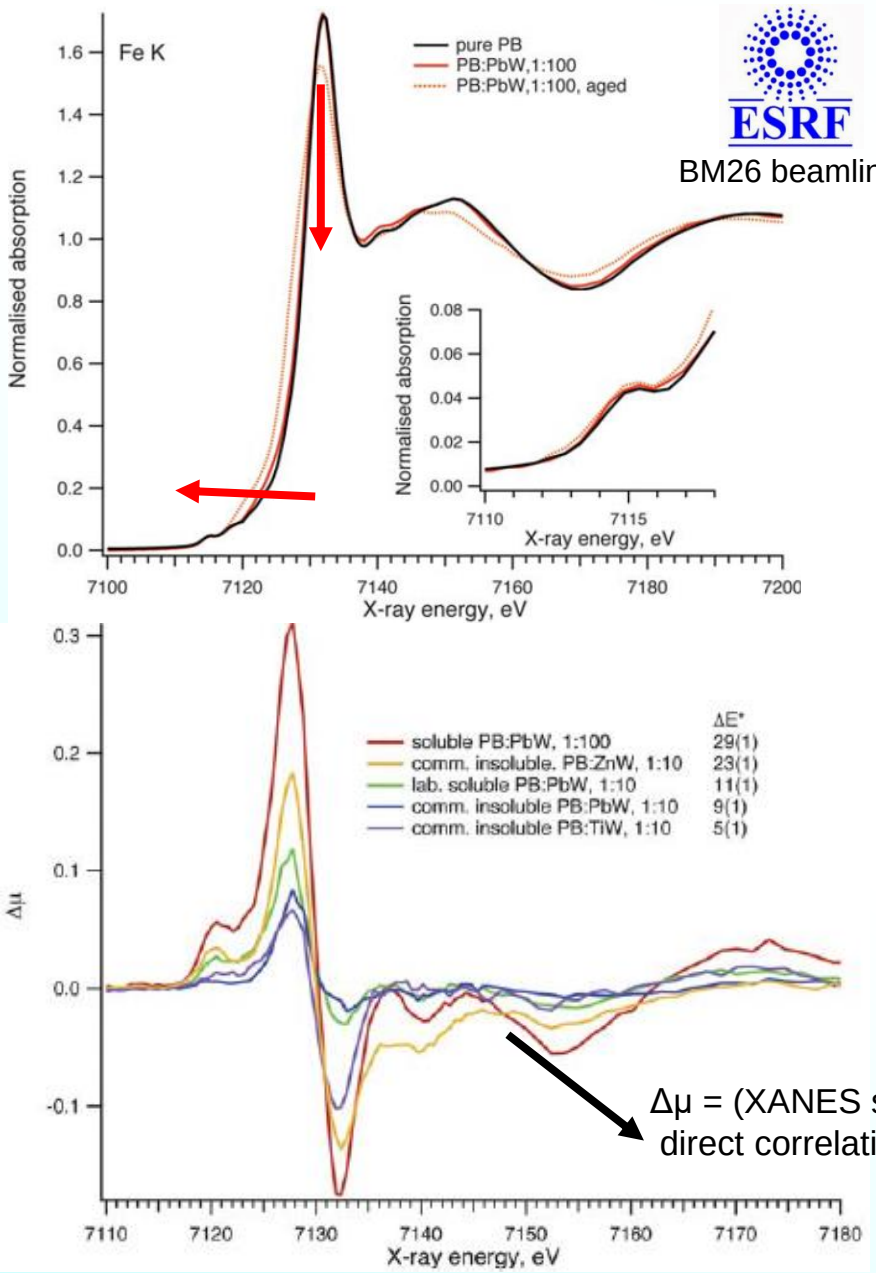

ESRF

BM26 beamline

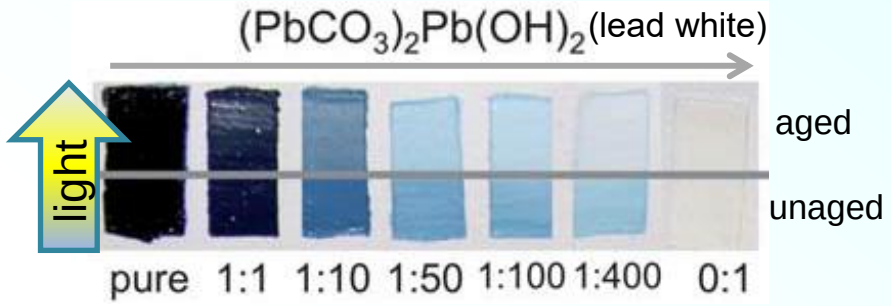

- ***Fading*** due to a Fe(III)→Fe(II) reduction (in the XAS spectrum: decreasing of the intensity of the white line and shift of the absorption edge towards lower energies).
- Disruption of the intervalent electron transfer Fe(II)-C-Fe(III).
- Decrease in the Fe coordination number in the second and third shell that lead to a weakening of the intervalent Fe(II)/Fe(III) charge transfer.
- The fading is influenced by the nature and amount of the white pigment.

$\Delta\mu$ = (XANES spectrum$_{unaged}$-XANES spectrum$_{aged}$): direct correlation with the total colour change (ΔE^*)

* L. Samain et *al.*, J. Anal. At. Spectrom. 26 (2011) 930-941.

Smalt discoloration

- ***Smalt*** : blue pigment commonly used by artists between the 16th and 18th centuries. It is a potash glass in which the color stems from cobalt ions in the divalent oxidation state.
- XAS investigations of micro-samples taken from paintings and artificially aged model samples have established the alteration mechanism of this pigment.

analytical chemistry

Anal. Chem. 2011, 83, 5145–5152 ARTICLE

pubs.acs.org/ac

Investigation of the Discoloration of Smalt Pigment in Historic Paintings by Micro-X-ray Absorption Spectroscopy at the Co K-Edge

Laurianne Robinet,*,† Marika Spring,‡ Sandrine Pagès-Camagna,§ Delphine Vantelon,∥ and Nicolas Trcera∥

JAAS *J. Anal. At. Spectrom.*, 2012, **27**, 1941–1948

Discoloration of the smalt pigment: experimental studies and *ab initio* calculations†

Ilaria Cianchetta,[a] Ivan Colantoni,[b] Fabio Talarico,*[c] Francesco d'Acapito,[d] Angela Trapananti,[d] Chiara Maurizio,[e] Simona Fantacci[f] and Ivan Davoli[b]

Co K-edge XAS (XANES/EXAFS) analysis*

LUCIA beamline
focusing optics: KB mirrors
beam size: 4 × 2 μm^2
SDD detector

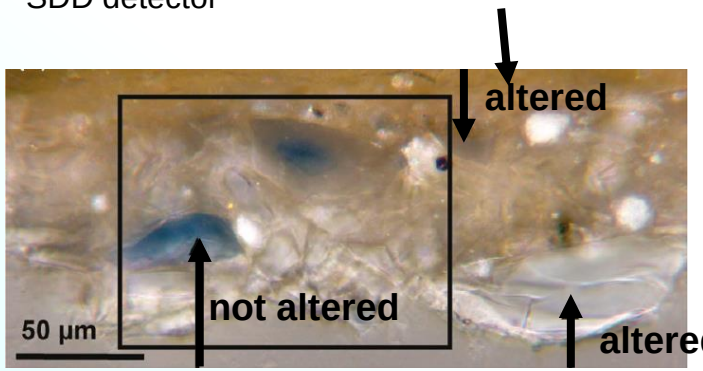

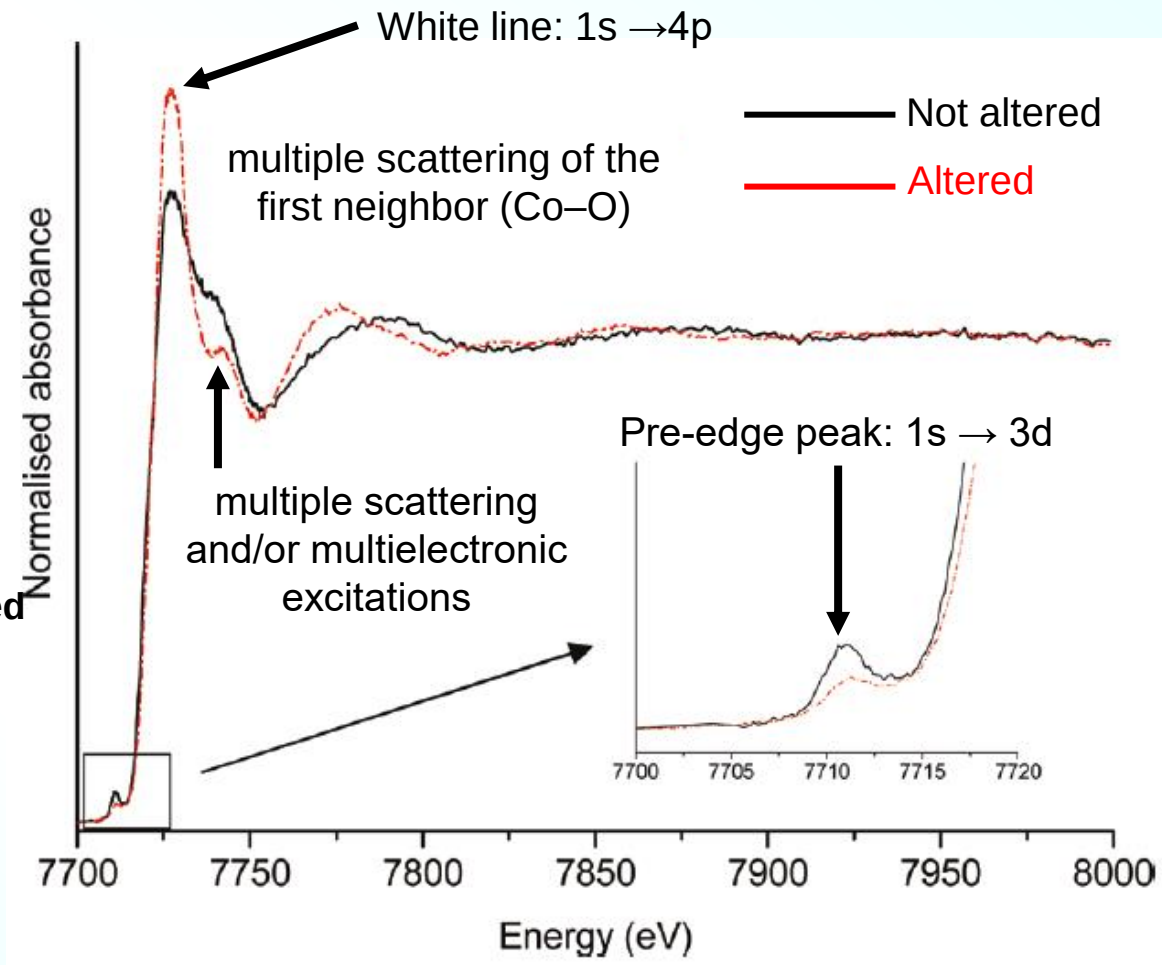

➢***Discoloration*** due to a change in the local environment of Co^{2+} from tetrahedral (blue) to octahedral (pink) while the leaching of K^+ takes place.
The process does not involve modifications of the oxidation state of the cobalt ion.

*Figures re-adapted from L. Robinet *et al.,* Anal. Chem. 83 (2011) 5145–5152.

Color changes in paintings: alteration of yellow pigments

Cr K-edge XAS analysis for the study of the darkening of chrome yellows

Darkening of chrome yellows ($PbCr_{1-x}S_xO_4$)

- Characterized by low photochemical stability with tendency to lose their original brilliant yellow color.


Bank of the Seine (F293, mid May-late July 1887, Van Gogh Museum)


Falling leaves (Les Alyscamps) (F486, November 1888, Kröller-Müller Museum)


The bedroom (F482, October, 1888, Van Gogh Museum)

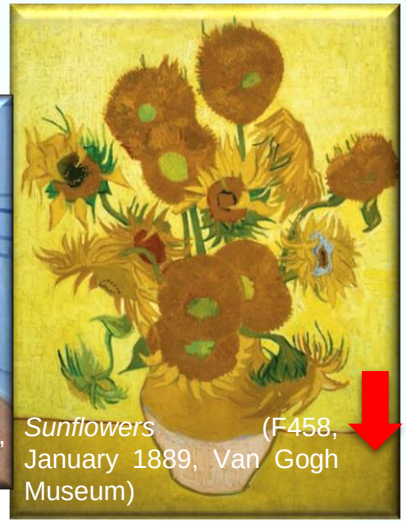
Sunflowers (F458, January 1889, Van Gogh Museum)

$[SO_4^{2-}]$ $PbCr_{1-x}S_xO_4$

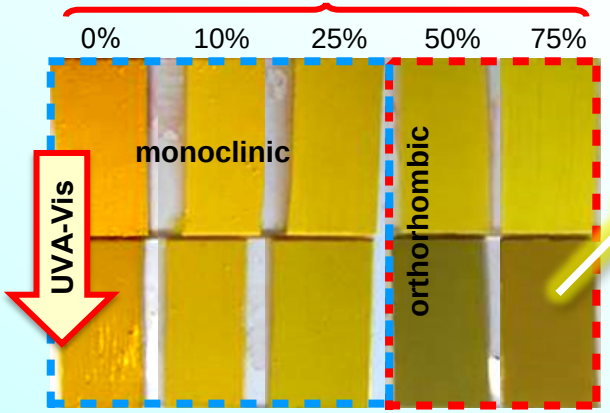

Photochemically aged mock-up paints

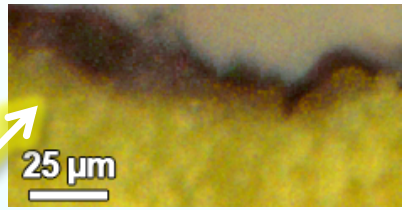

Thin alteration layer (thickness: <10 µm)

- ***Darkening due to a (photo) reduction process:***

  $Cr^{VI} \rightarrow Cr^{III}$

- ***Cr-reduction depends on:***

  a) Cr:S stoichiometry
  b) Crystalline structure
  c) Binding medium
  d) Solubility of lead chromate-type

*L. Monico *et al., Anal. Chem.* 83 (2011) 1214–1223; L. Monico *et al., Anal. Chem.* 83 (2011) 1224-1231; L. Monico *et al., Anal. Chem.* 85 (2013) 860-867; L. Monico *et al., Anal. Chem.* 86 (2014) 10804–10811; L. Monico *et al., JAAS* 30 (2015) 613-626; L. Monico *et al., JAAS* 30 (2015) 1500-1510; L. Monico *et al., Angew. Chem. Int. Ed.* 54 (2015) 13923-13927; L. Monico *et al., ACS Omega* 4 (2019) 6607-6619.

Cr speciation investigations: Cr K-edge XANES

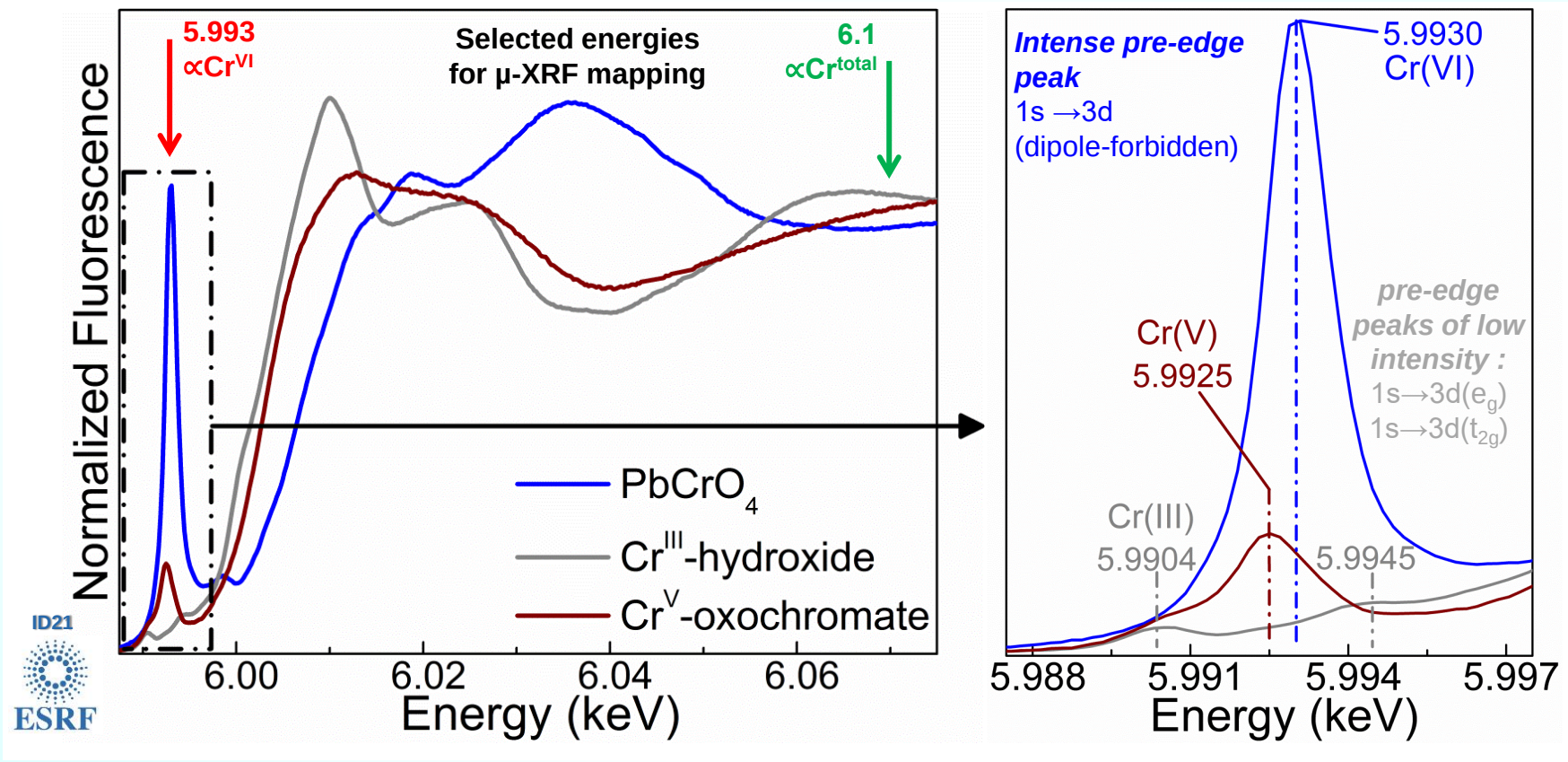

- **Cr(VI) compounds:** non-centrosymmetric tetrahedral coordination.
- **Cr(III) compounds:** centrosymmetric octahedral geometry.
- Pre-edge peak area proportional to the relative amount of Cr(VI).
- Shift of the absorption edge position towards higher energies: ***increase of the valency*** of the absorbing atom and/or of the ***electronegativity*** of the nearest neighbour atoms.
- Identification of specific reduced Cr-compounds challenging, when different Cr-species are co-present.

Van Gogh Museum Amsterdam

CHARISMA

IPERION CH

Van Gogh's Sunflowers (Amsterdam version)

Angewandte Chemie

Evidence for Degradation of the Chrome Yellows in Van Gogh's *Sunflowers*: A Study Using Noninvasive In Situ Methods and Synchrotron-Radiation-Based X-ray Techniques

Letizia Monico, Koen Janssens, Ella Hendriks, Frederik Vanmeert, Geert Van der Snickt, Marine Cotte, Gerald Falkenberg, Brunetto Giovanni Brunetti, and Costanza Miliani*

Angew. Chem. **2015**, *127*, 14129–14133

Chemical Mapping by Macroscopic X-ray Powder Diffraction (MA-XRPD) of Van Gogh's *Sunflowers*: Identification of Areas with Higher Degradation Risk

Frederik Vanmeert, Ella Hendriks, Geert Van der Snickt, Letizia Monico, Joris Dik, and Koen Janssens*

Angew. Chem. Int. Ed. **2018**, *57*, 7418–7422

AUP Amsterdam University Press

Cr speciation analyses: aged paint mock-ups & original paint micro-samples

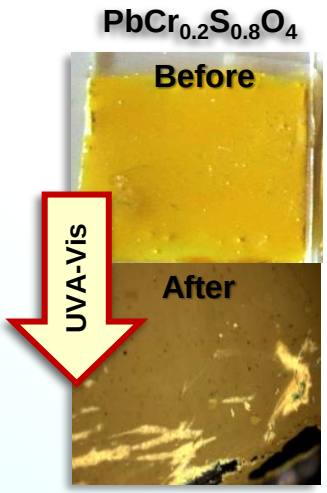

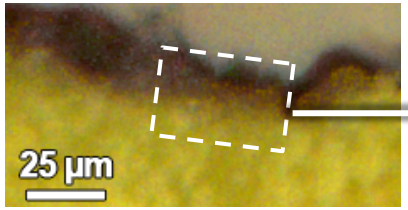

Thin section (thickness: ~5 µm)

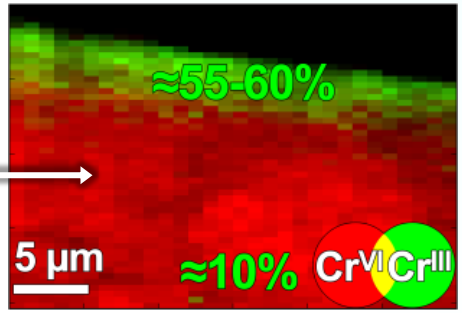

step size (h×v): 0.8×0.3 µm²
dwell time: 100 ms/pixel
Energy: 5.993-6.1 keV

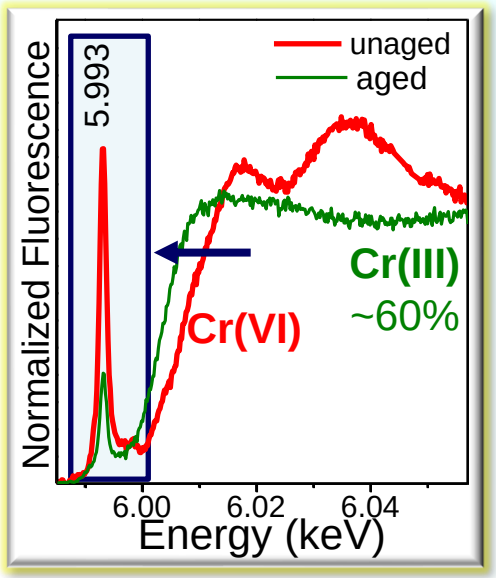

Sunflowers (F458, January 1889, Van Gogh Museum)

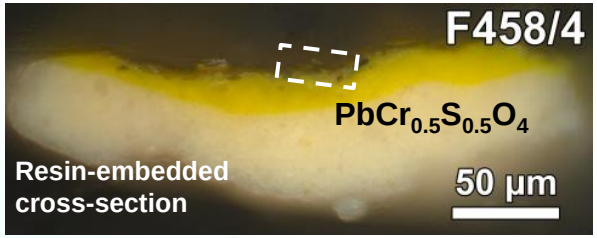

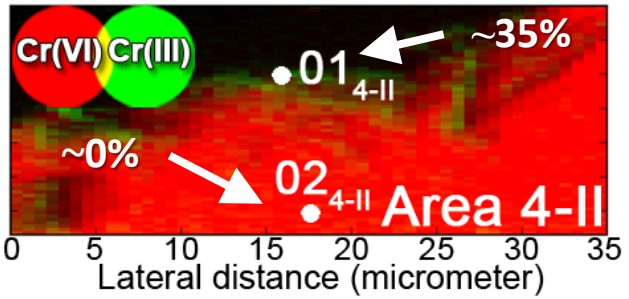

step size (h×v): 0.7×0.2 µm²
dwell time: 100 ms/pixel
Energy: 5.993-6.1 keV

*L. Monico *et al., Anal. Chem.* 85 (2013) 860-867; L. Monico *et al., JAAS* 30 (2015) 1500-1510; L. Monico *et al., Angew. Chem. Int. Ed.* 54 (2015) 13923-13927.

Maia and SSD-detector based microprobe systems: The Bedroom*

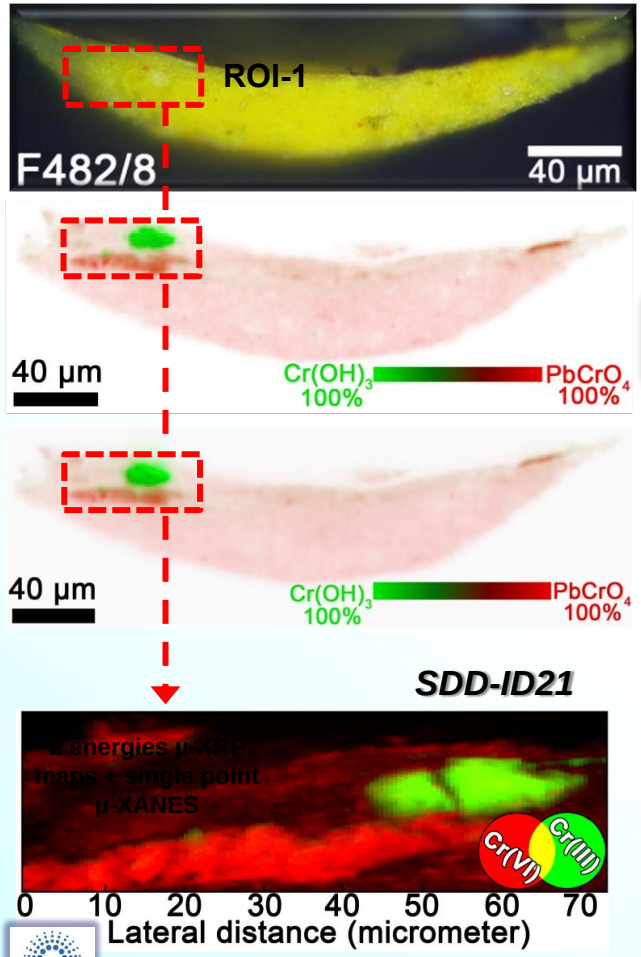

Maia-XFM

Australian Synchrotron

Maia-P06

DESY

The Bedroom (V. van Gogh, October 1888, Van Gogh Museum, Amsterdam).

↑ Faster acquisition time (factor of 10^2 -10^3 shorter per energy scan)
↑ More representative datasets (analysis of larger areas- larger n. of XANES spectra)
↑ Lower fluences (2-3 order of magnitude; decreasing of beam damage probability)

↓ Lower lateral resolution (~0.7-2 µm)
↓ Lower spectral energy resolution
↓ Stage platform less stable (Y drift correction /re-alignment)
↓ Lower fluences (lower signal to noise ratio)

Microprobe system	Map size (h×v) (µ²)	Pixel size (h×v) (µm²)	Pixel total number	Dwell time (ms/pixel)	Acquisition time (min)	Absolute photon flux (ph/s)	fluence (ph/µm²)
Maia-P06	300×80	1×1	2.4×10^4	3	210	9×10^8	8×10^8
Maia-XFM	300×80	1×1	2.4×10^4	0.99	130	2.1×10^8	2.6×10^7
SDD-ID21	73.8×22.6	0.6×0.2	1.3899×10^4	150-300	108	1.7×10^8	3.3×10^7

* L. Monico *et al.*, *JAAS* 30 (2015) 613-626.

Cr K-edge XANES spectroscopy in total electron yield (TEY) & total X-ray fluorescence (XFY) modes

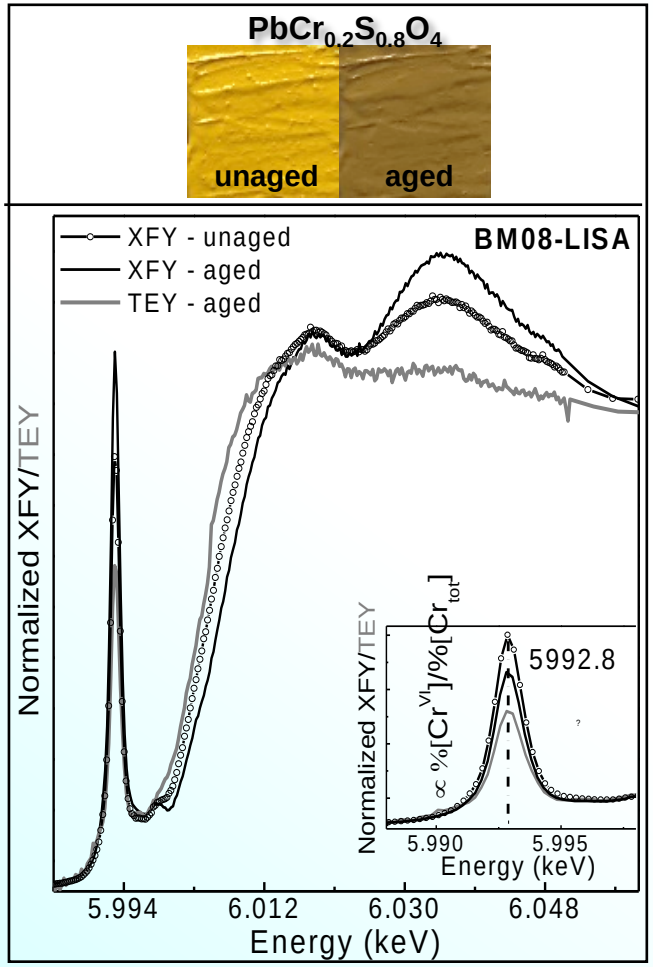

TEY mode: analysis directly from the surface (no thin section preparation) and sensitive to uppermost 1-2 micromoters of the paint stratigraphy

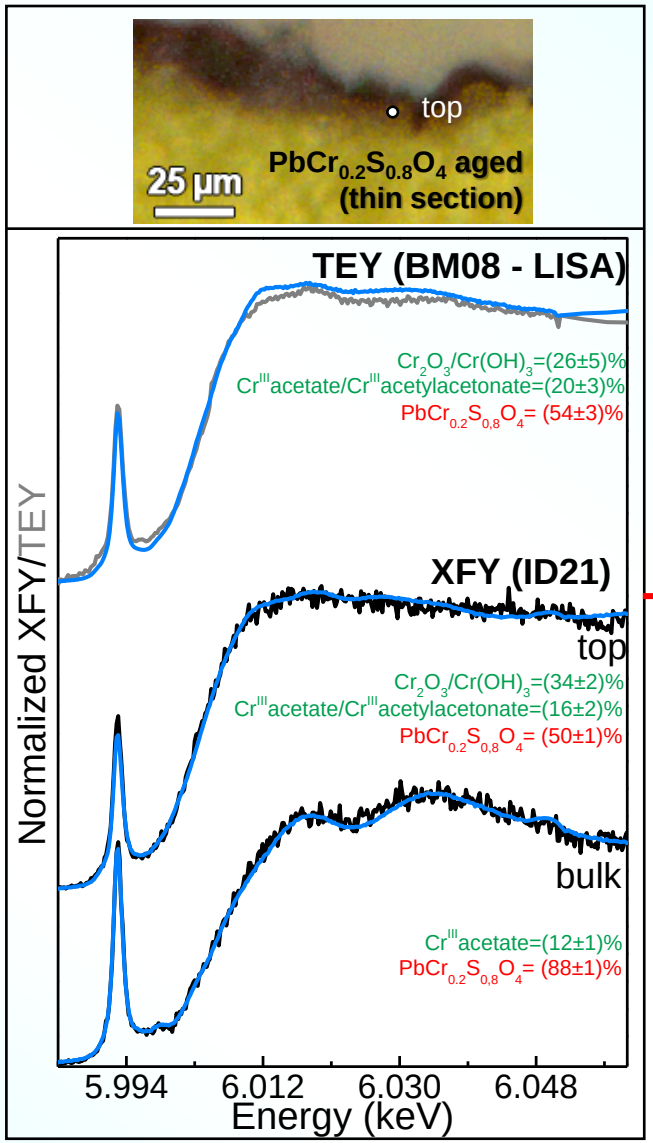

Good agreement between the XFY mode data recorded from the darkened layer of the cross-section and the TEY mode collected from the alterd paint surface of a fragment

* L. Monico *et al.*, *Nuclear Instruments and Methods in Physics Research B 539 (2023)141–147.*

Radiation damage on cultural heritage materials: further readings

Trends in Analytical Chemistry 66 (2015) 128–145

Contents lists available at ScienceDirect

Trends in Analytical Chemistry

journal homepage: www.elsevier.com/locate/trac

Mitigation strategies for radiation damage in the analysis of ancient materials

Loïc Bertrand [a,b,*], Sebastian Schöeder [b], Demetrios Anglos [c,d], Mark B.H. Breese [e], Koen Janssens [f], Mehdi Moini [g], Aliz Simon [h,i]

Trends in Analytical Chemistry 164 (2023) 117078

Contents lists available at ScienceDirect

Trends in Analytical Chemistry

journal homepage: www.elsevier.com/locate/trac

Practical advances towards safer analysis of heritage samples and objects

Loïc Bertrand [a,*], Sebastian Schöder [b], Ineke Joosten [c], Samuel M. Webb [d], Mathieu Thoury [e], Thomas Calligaro [f], Étienne Anheim [g], Aliz Simon [h]

Safe analysis conditions of chrome yellows by SR X-ray methods

analytical chemistry

pubs.acs.org/ac Article

Damages Induced by Synchrotron Radiation-Based X-ray Microanalysis in Chrome Yellow Paints and Related Cr-Compounds: Assessment, Quantification, and Mitigation Strategies

Letizia Monico,* Marine Cotte, Frederik Vanmeert, Lucia Amidani, Koen Janssens, Gert Nuyts, Jan Garrevoet, Gerald Falkenberg, Pieter Glatzel, Aldo Romani, and Costanza Miliani

Cite This: *Anal. Chem.* 2020, 92, 14164−14173 Read Online

- ***ID26:*** Cr-Kβ XES/ Cr K-edge high-energy resolution fluorescence detected (HERFD)-XANES
- ***ID21:*** µ-XRF/Cr K-edge µ-XANES
- ***P06:*** µ-XRD

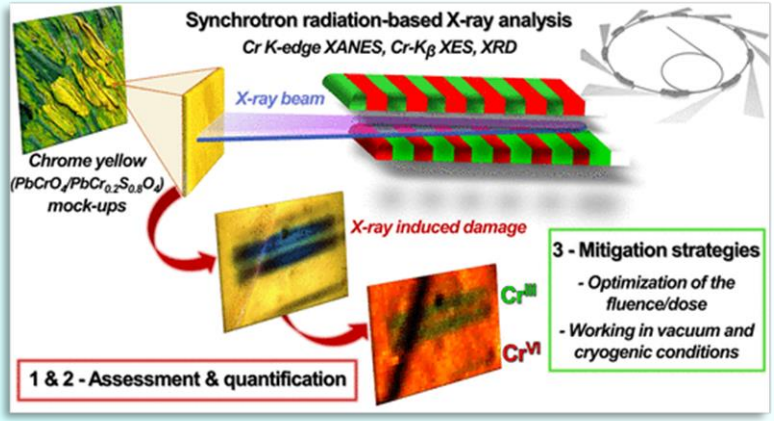

light-fast $PbCrO_4$

oil *acrylic*

powder

light-sensitive $PbCr_{0.2}S_{0.8}O_4$

oil *acrylic*

powder

Cr-Kβ XES/ Cr K-edge HERFD-XANES (ID26)*

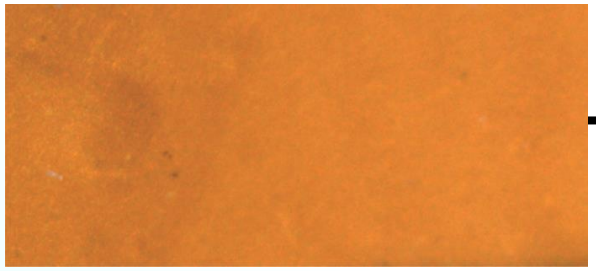

$PbCrO_4$-oil

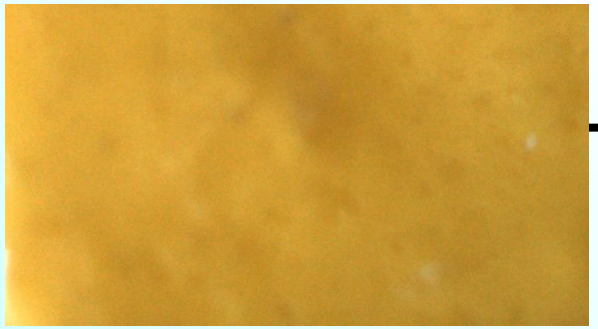

$PbCr_{0.2}S_{0.8}O_4$-oil

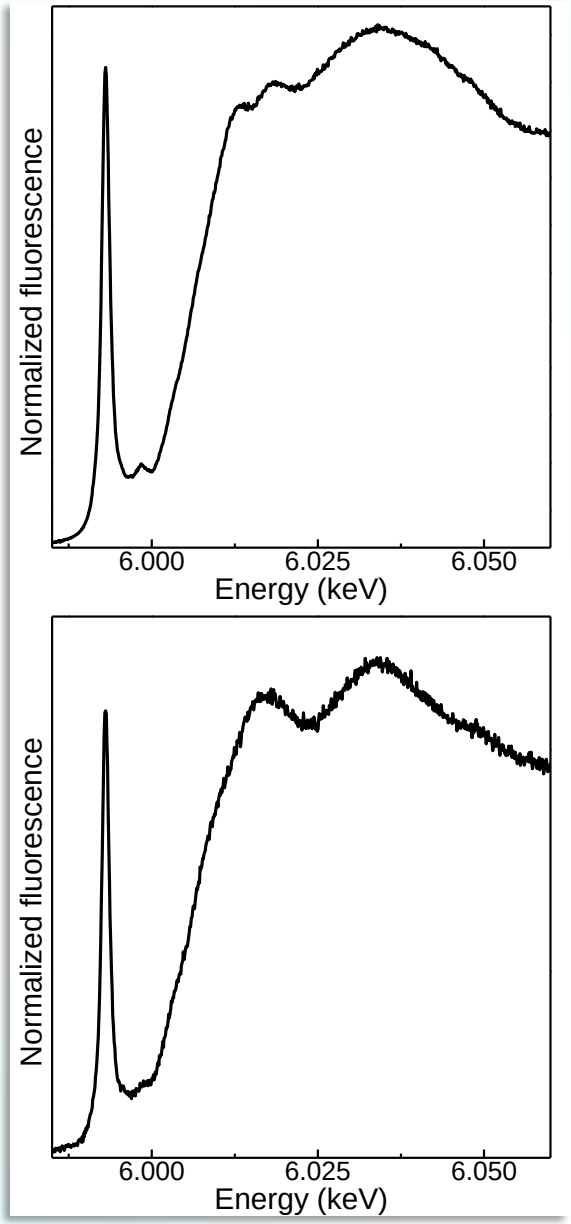

ESRF
ID26

***Before Cr Kβ XES*:**
Cr^{VI}-species

*L. Monico et al., *Anal. Chem.* 92 (2020) 14164-14173.

Cr-Kβ XES/ Cr K-edge HERFD-XANES (ID26)*

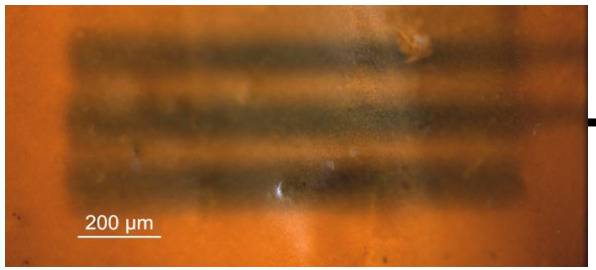

$PbCrO_4$-oil

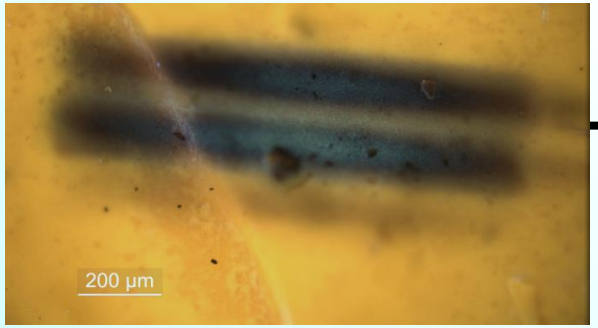

$PbCr_{0.2}S_{0.8}O_4$-oil

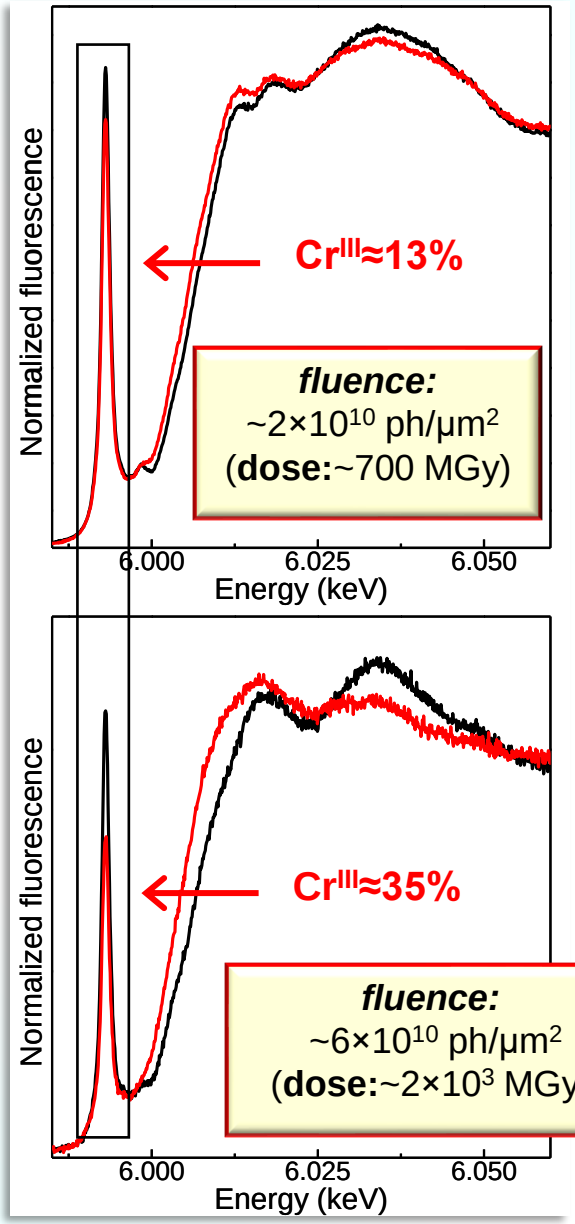

ESRF
ID26

***Before Cr Kβ XES*:**
Cr^{VI}-species

***After Cr Kβ XES*:**
SR X-ray induced reduction process

*L. Monico et al., *Anal. Chem.* 92 (2020) 14164-14173.

Cr-speciation mapping (ID21)*

ID21

ESRF

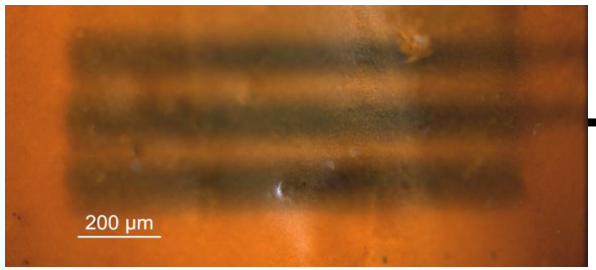

$PbCrO_4$-oil

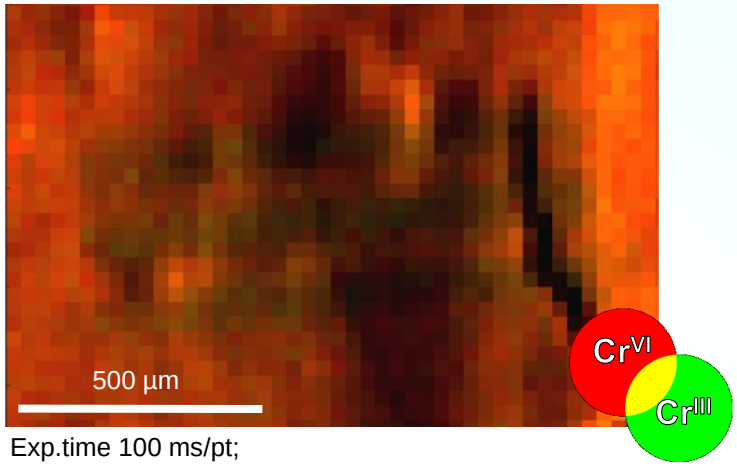

Exp.time 100 ms/pt;
Size (h×v):1.5×1.2 mm²
Step: 30×30 µm²

"Burnt" areas: Cr-reduction

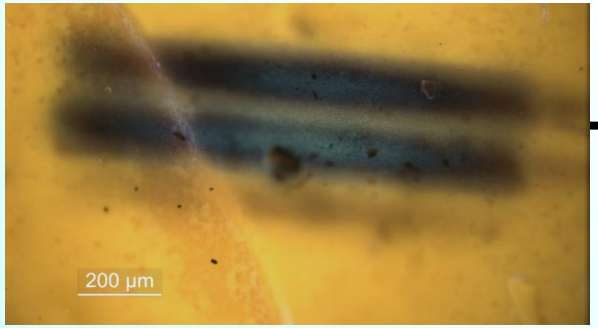

$PbCr_{0.2}S_{0.8}O_4$-oil

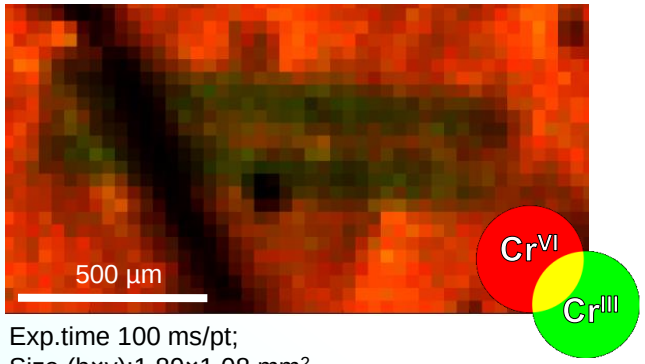

Exp.time 100 ms/pt;
Size (h×v):1.89×1.08 mm²
Step: 30×30 µm²

*L. Monico et al., *Anal. Chem.* 92 (2020) 14164-14173.

Cr K-edge μ-XANES (ID21): effect of S content*

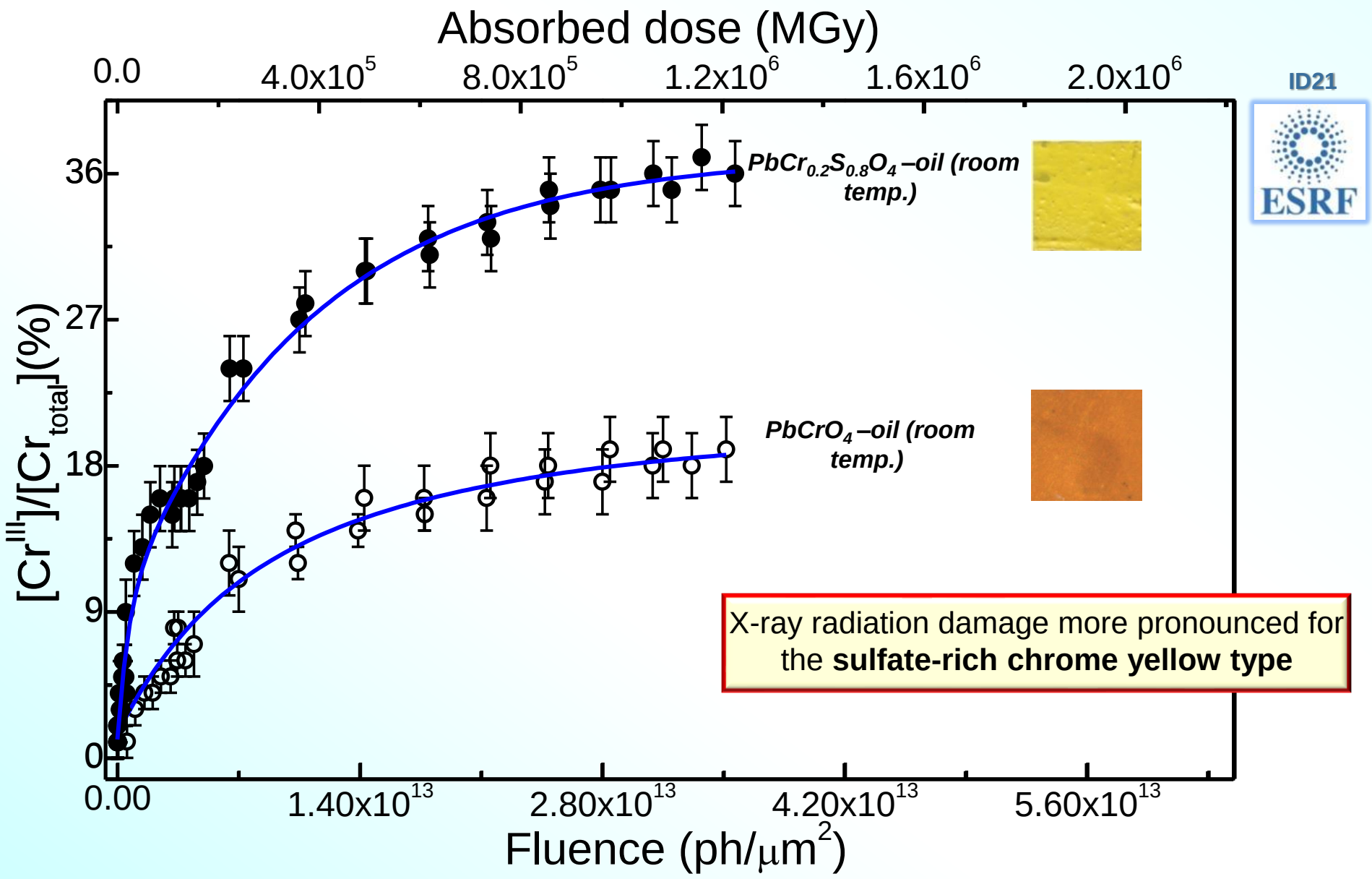

*L. Monico et al., *Anal. Chem.* 92 (2020) 14164-14173.

Cr K-edge μ-XANES (ID21): effect of the binder*

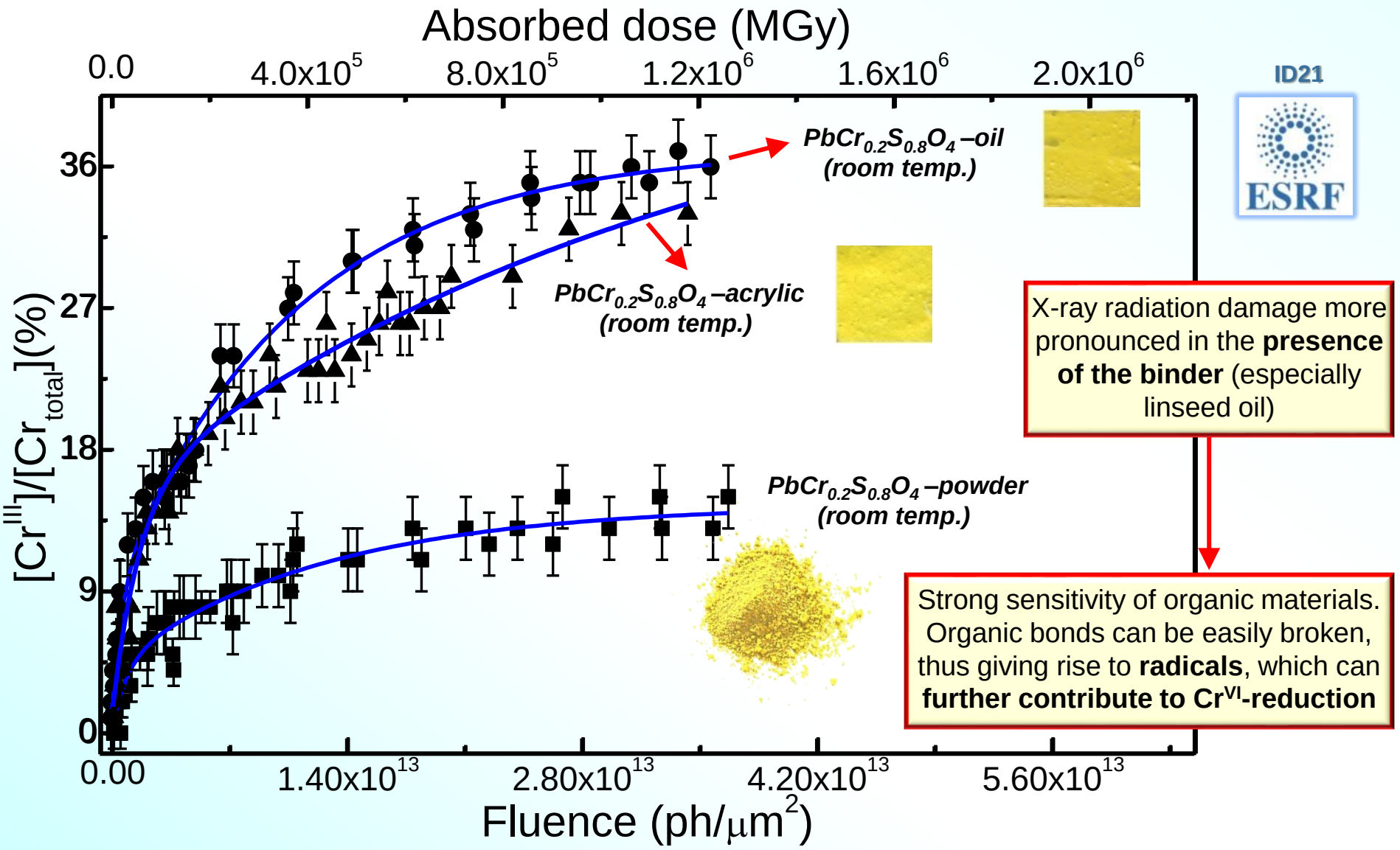

*L. Monico et al., *Anal. Chem.* 92 (2020) 14164-14173.

μ-XRD (P06-PETRA III)*

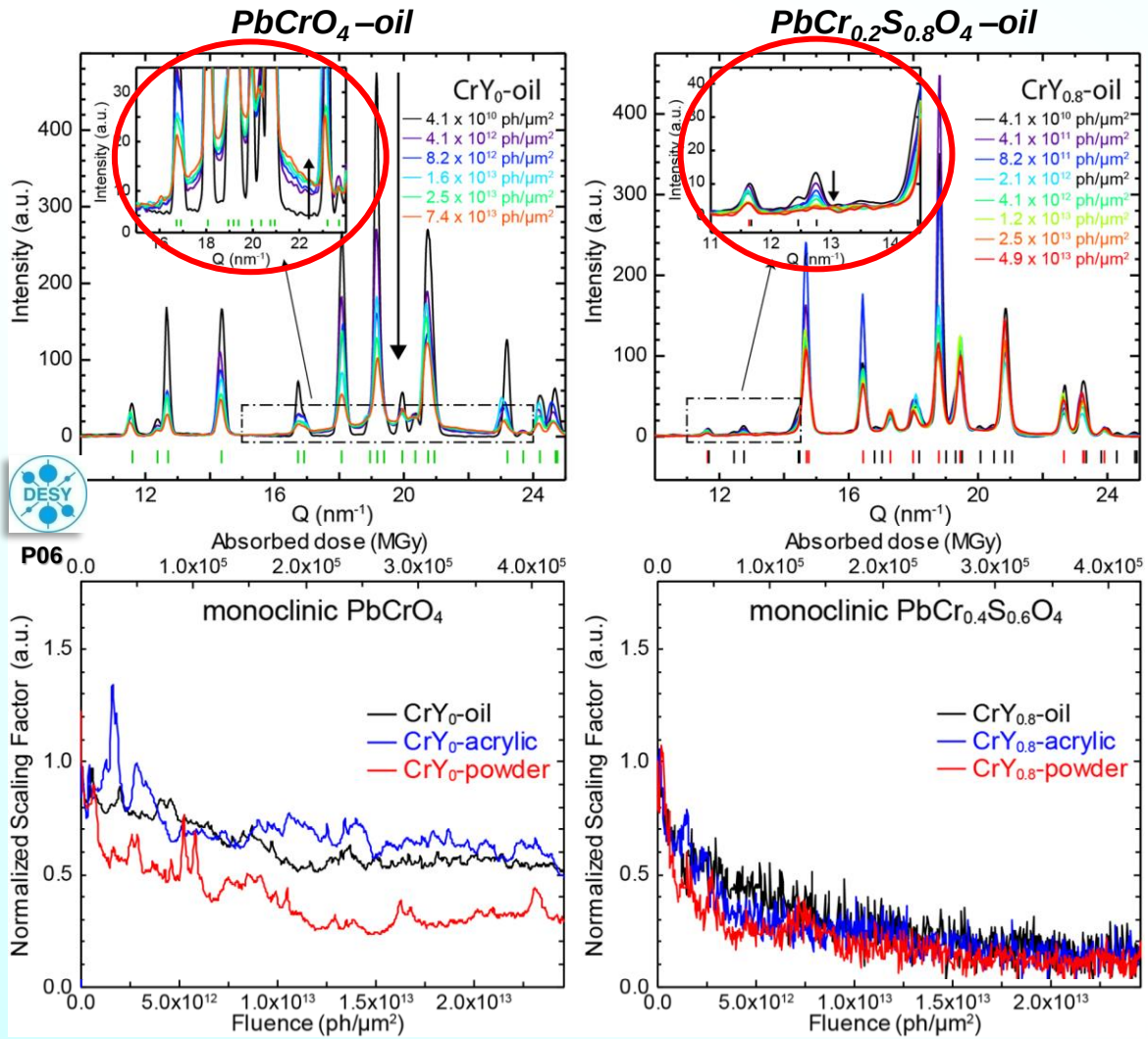

- Formation of an amorphous phase (clearly visible for $PbCrO_4$ –oil);
- Loss of crystalline structure (decreasing of the intensity of the diffraction signals);
- It is more pronounced for the sulfate-richer phases.

Cr-speciation mapping

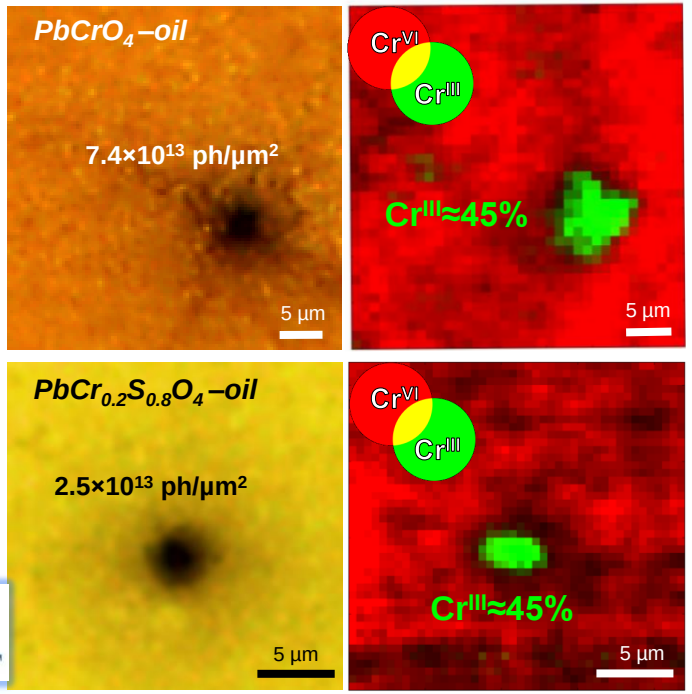

ID21

*L. Monico et al., *Anal. Chem.* 92 (2020) 14164-14173.

Mitigation strategies: optimization of the fluence/dose & vacuum conditions *

- **Different extent** of **photo-induced reduction** for **similar doses** (different fluence/dose threshold);

Beamline	Energy (keV)	Fluence threshold (ph/µm²)	Absorbed dose threshold (MGy)	Vacuum
ESRF-ID21	~6	~5×10^{11}	~2×10^{4}	Yes
ESRF-ID26	~6	~10^{8}	~10	No
DESY-P06	21	~$1\text{-}2\times10^{11}$	~$2\text{-}4\times10^{3}$	No

- **Adapt time** to stay below the established threshold value (fast-data acquisition – ID26 beamline);
- **Decreasing the flux** of the incoming beam (e.g., using attenuators of different thickness) as long as an adequate signal-to-noise-ratio is maintained;
- **Defocusing the beam** to minimize the fluence/dose to the sample, but sometimes at the expense of spectral resolution (e.g., XES analysis).
- **Vacuum conditions:** explain the lower Cr^{III}-abundances obtained at ESRF-ID21;
- Such sample environment may contribute to **indirectly slowing down the Cr-reduction** due to the **absence/neglectable content of air gases (e.g., O_2) and moisture,** that favor the oxidative degradation of the binding medium.

*L. Monico et al., *Anal. Chem.* 92 (2020) 14164-14173.

Mitigation strategies: lowering the temperature*

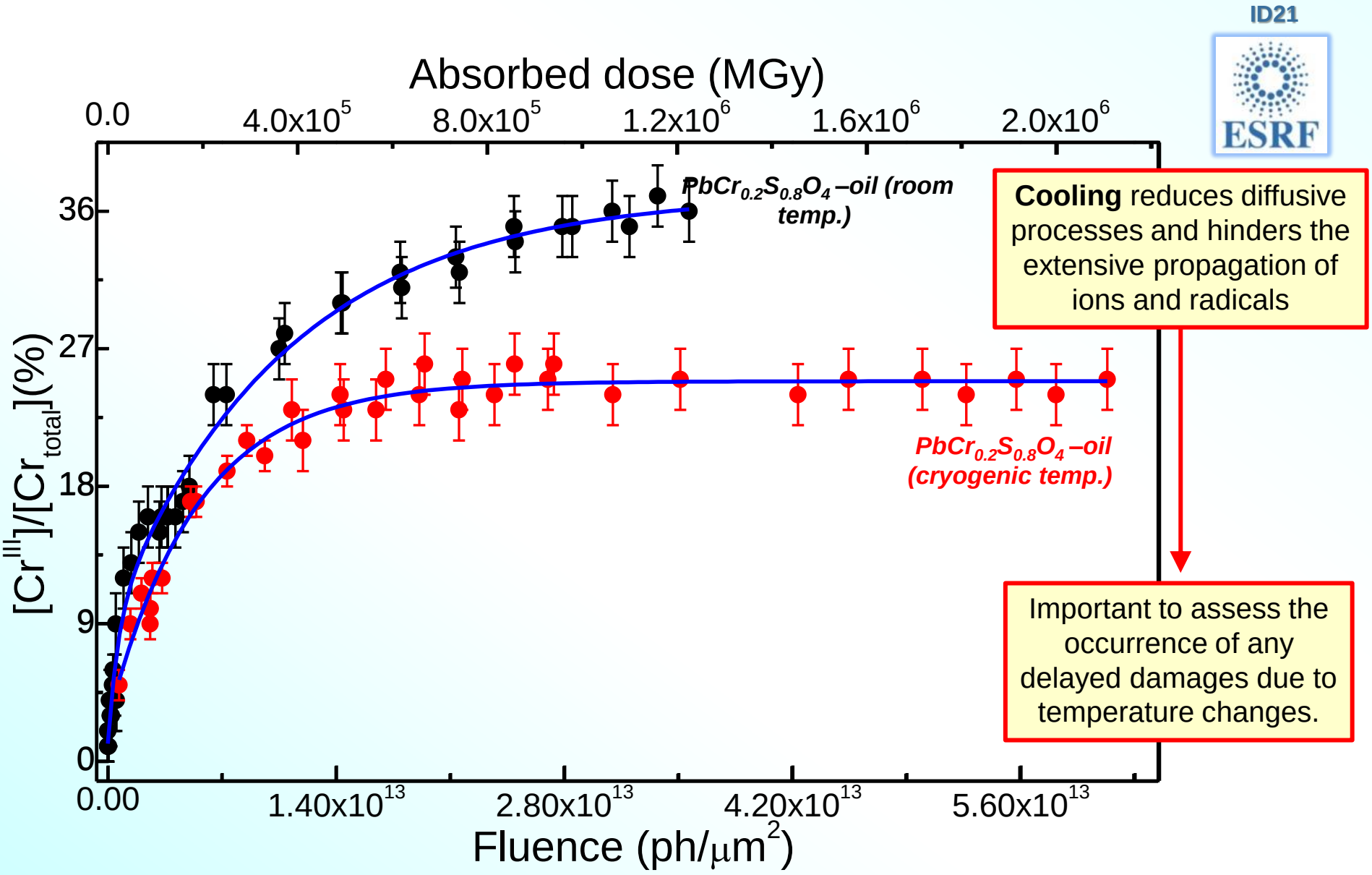

*L. Monico et al., *Anal. Chem.* 92 (2020) 14164-14173.

THE “HISTORICAL MATERIALS” BLOCK ALLOCATION GROUP: A COMMUNITY ACCESS

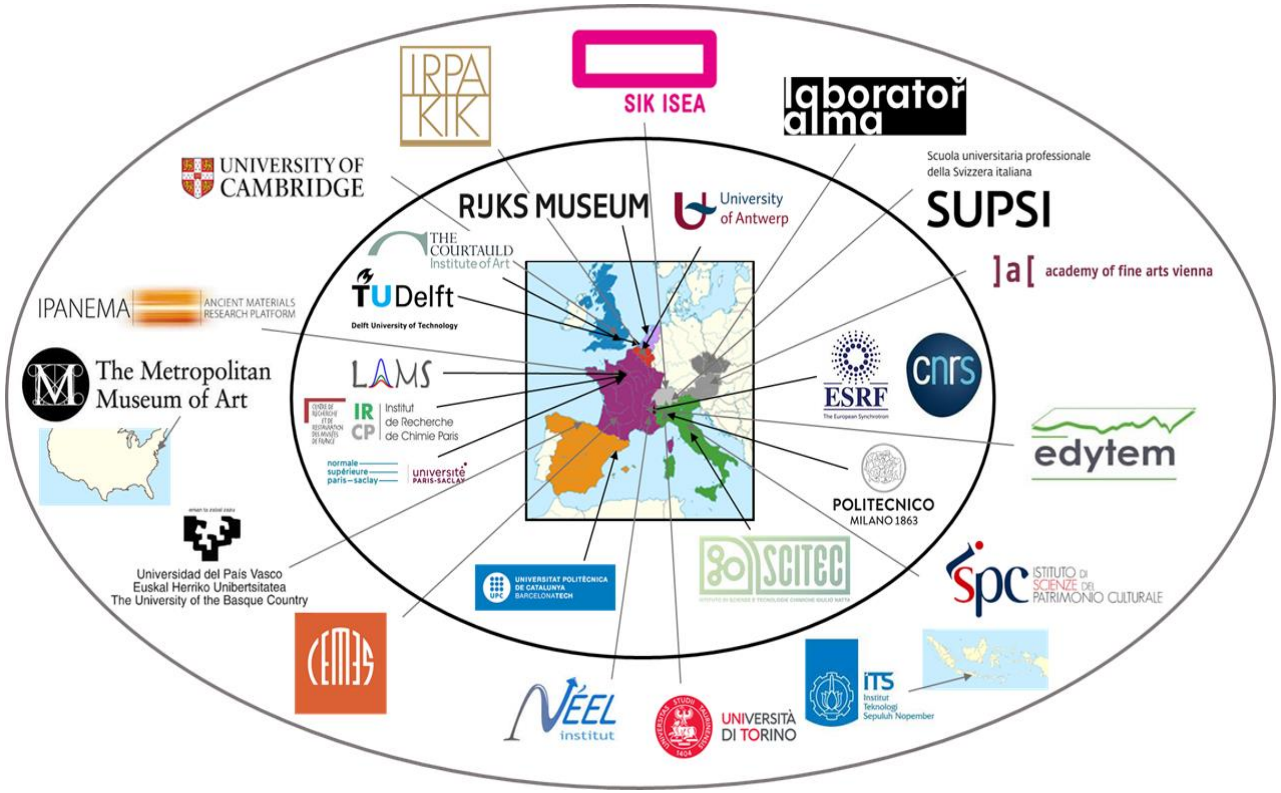

First ring: partners of the initial BAG proposal
Second ring: indirect partners through collaborations

Access to
µ-XRD mapping (ID13, 4 days)
HR-XRD (ID22, 3 days)
every 6 months for 2 years

Beamtime shared between the partners
Synergy and mutual support
A very good training programme

https://www.esrf.fr/BAG/HG172

Heritage-bag@esrf.fr

STREAMLINE

The European Synchrotron | ESRF

FROM STANDARD ACCESS MODELS TO BLOCK ALLOCATION GROUP (BAG) ACCESS

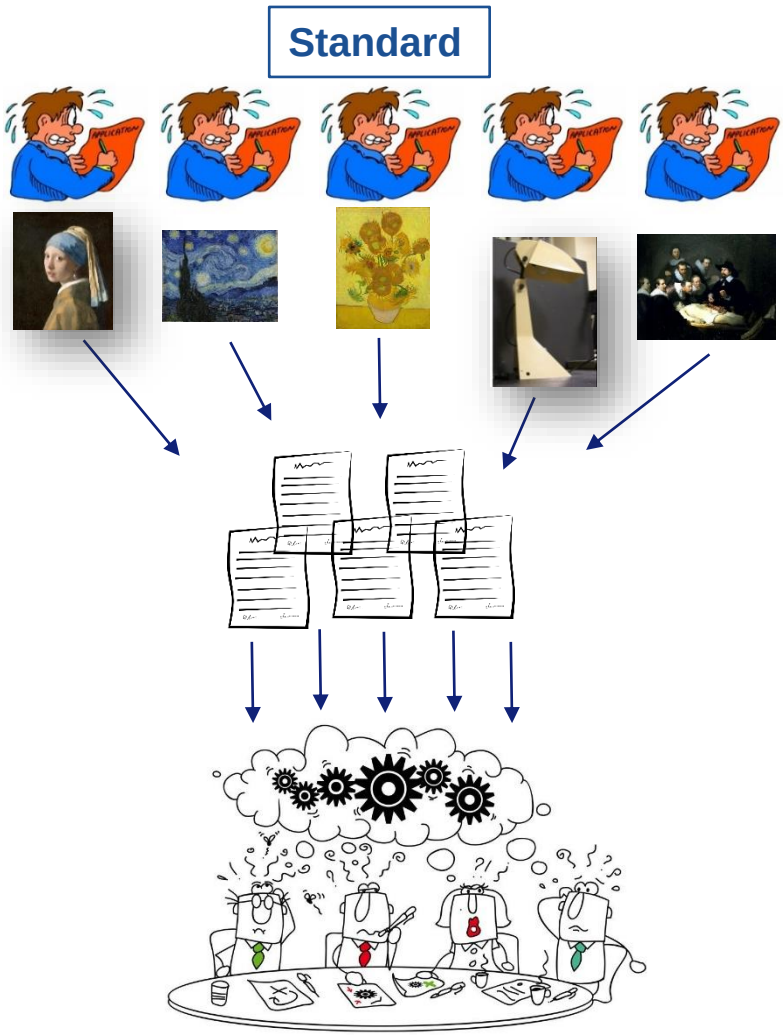

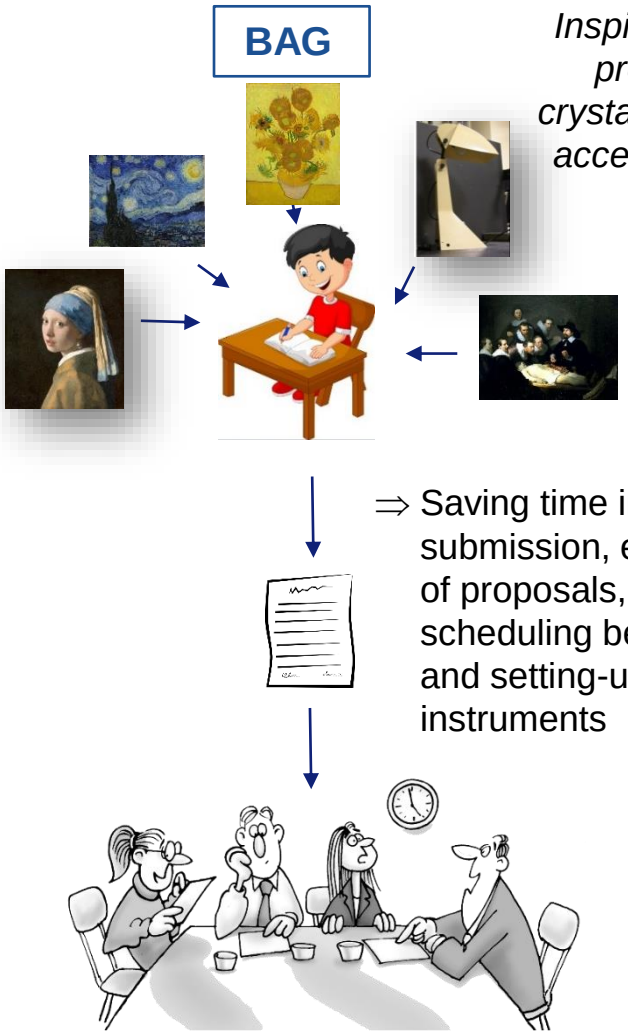

Inspired from proteins crystallography access mode

⇒ Saving time in submission, evaluation of proposals, scheduling beamtime and setting-up of instruments